

Diplomarbeit

zum Thema

Nucleation Experiments on Ices in Respect of Atmospheric Chemistry

ausgeführt am
Institut für Materialchemie
der Technischen Universität Wien

unter der Anleitung von
Ao.Univ.Prof. Dipl.-Chem. Dr.rer.nat. Hinrich Grothe

durch

Baloh Philipp
Matrikelnr.: 0125613
Clessgasse 89, 1210 Wien

Wien, am 15. 12. 2010

Philipp Baloh

Zusammenfassung

Wolken beeinflussen das Wetter und die Temperaturen auf unserer Erde auf verschiedenste Weise. Spätestens seit dem Report des Intergovernmental Panel on Climate Change 2007 IPCC (2007) rückte das Thema Klimawandel stark ins Interesse der Öffentlichkeit. Abseits aller Kontroversen die das Thema aufwirft, bietet der Report gut aufgearbeitete Daten, welche zeigen, in welchen Bereichen weitere Aufklärung notwendig ist, wenn man sich dem Verständnis des Klimasystems annähern möchte. Eine wichtige Größe im Klimasystem ist die Strahlungsbilanz der Erde. Diese bezeichnet die Bilanz der in das System Erde eingehenden und ausgehenden Strahlung. Zur Erwärmung oder Abkühlung tragen Prozesse wie Reflexion und Absorption an der Erdoberfläche oder auch in der Atmosphäre bei. Bei der Aufstellung dieser Daten im IPCC-Report sieht man, dass das Wissen über die Strahlungsbilanz bei Aerosolen und Wolken mit einer sehr großen Unsicherheit behaftet ist. Diese Unsicherheit wurzelt mitunter in der messtechnisch schwierigen Erreichbarkeit von Wolken. Um diese Lücke zu schließen, werden Modelle von Wolken benutzt. Diese simulieren im Labormaßstab wolkenähnliche Verhältnisse, um daran Messungen durchzuführen.

Die vorliegende Arbeit beschäftigt sich einerseits mit dem Gefrierverhalten von unabhängigen Wassertropfen in einem Modell in Hinblick auf Cirrus-Wolken. Andererseits wurden spektroskopische Untersuchungen an Salpetersäurehydraten vorgenommen, welche eine wichtige Rolle bei der Bildung von Polarstratosphärischen-Wolken spielen.

Das verwendete Modell für die Cirrus-Wolken bestand aus einer Emulsion aus Wasser in einem Öl, um sehr kleine voneinander unabhängige Tröpfchen zu simulieren. Der wässrigen Phase wurden verschiedene Konzentrationen von Zitronensäure zugesetzt, um den Einfluss einer organischen Säure auf das Gefrierverhalten der Wassertropfen zu untersuchen. Folgende Analysemethoden wurden angewandt, um Informationen über das Eis zu gewinnen:

- Röntgendiffraktion bei tiefen Temperaturen (Cryo-XRD)
- Ramanspektroskopie bei tiefen Temperaturen
- Elektronenmikroskopie unter Gasphase bei tiefen Temperaturen (Cryo-ESEM)

Für die Messungen am Ramanspektrometer wurde eine neue Tieftemperaturzelle entwickelt, mit welcher die Möglichkeit besteht, die gewünschten Temperaturbedingungen konstant einzustellen. Im Rahmen der Untersuchungen hat sich gezeigt, dass Zitronensäure das Gefrierverhalten von Wassereis unter troposphärischen Bedingungen stark beeinflusst. So kommt üblicherweise bei den auf der Erde herrschenden Bedingungen nur hexagonales Eis I_h als Standardmodifikation vor, was sich etwa in der Sechsstrahligkeit von Schneeflocken widerspiegelt. Die Zitronensäure bedingt nun eine Störung dieser Struktur und es wird, wie es in der Literatur bei Murray (2008a) schon beschrieben ist, vermehrt kubisches Eis I_c gebildet. Dieser, erst seit kurzem bekannte Effekt konnte mittels XRD gut beobachtet werden. Weiters wurde erstmals eine Verminderung der Kristallitgrößen bei steigender Zitronensäurekonzentration beobachtet, was auf eine Hemmung des Kristallwachstums bei höheren Zitronensäurekonzentrationen schließen lässt.

Fänden ähnliche Prozesse auch an Wolkenteilchen statt, wäre das eine mögliche Erklärung für Beobachtungen bei denen sich in Luftmassen keine Eiswolken bilden, obwohl die Temperatur schon lange unter die der Eisbildung gefallen ist ($\approx 220K$).

Die Zitronensäure selbst kommt in der Atmosphäre nur in sehr geringen Mengen vor, wurde jedoch hier als Modellsubstanz für andere Karbonsäuren verwendet, da sie in der Literatur sehr gut dokumentiert ist.

Als weiteres Thema dieser Arbeit wurden Salpetersäurehydrate mittels Inelastischer Neutronen Streuung (INS) untersucht. Salpetersäurehydrate spielen eine wichtige Rolle beim Bildungsmechanismus von Polarstratosphärischen-Wolken. Besonders Salpetersäuretrihydrat (NAT) und seine Phasen ($\alpha+\beta$ -NAT) sind diesbezüglich interessant, weshalb sie spektroskopisch untersucht wurden. Dabei konnten erstmals INS Spektren von α - und β - NAT aufgenommen und damit das in der Literatur beschriebene Phasendiagramm untermauert werden. Von Salpetersäuremonohydrat (NAM) konnten ebenfalls neue Spektren aufgenommen werden. Dieses besitzt aufgrund der hohen Salpetersäurekonzentration zwar wenig Relevanz für die Atmosphäre, wird aber gerne als Modellsubstanz verwendet, um beispielsweise Vibrationsspektren theoretisch zu berechnen, da es eine relativ einfache Einheitszelle besitzt. Beide Substanzen konnten zudem mit einem neuen Verfahren aus der amorphen Phase entwickelt werden.

Abstract

For the earth's climate system clouds are of major importance. On the one hand they can act as a cooling factor by reflecting parts of the solar radiation, and on the other hand they can cause warming by absorbing solar radiation and by trapping the outgoing blackbody radiation. These effects are not so well understood for making exact determinations about the overall radiation balance of the earth. In fact, clouds and aerosol particles are presented as one of the largest uncertainty factors of the radiation balance in the Report of the International Panel on Climate Change IPCC (2007). Therefore a great deal of research is directed to a better understanding of the aerosol effects. Homogeneous ice nucleation in aqueous solution droplets is one of the discussed research subjects as it is an important parameter for the formation of ice clouds. Ice nucleation may occur heterogeneously e.g. ice nucleation on dust particles or homogeneous without interference from other particles.

In this work two groups of reagents with atmospheric relevance were investigated. One topic was the investigation of emulsions containing aqueous droplets of citric acid as a model system for carboxylic acids in cirrus cloud droplets. The other topic was the hydrates of nitric acid, which play a role in the building mechanism of Polar Stratospheric Clouds.

For the investigations concerning the cirrus clouds, emulsions with different concentrations of citric acid were prepared and observed using the following methods:

- X-Ray Diffraction was carried out to gain information about the phase composition.
- Environmental Scanning Electron Microscopy(ESEM) was used to observe the morphology of the samples.
- Raman Spectroscopy was applied to get a look at the spectroscopic information of the droplets.

The model system showed certain interesting trends under atmospheric conditions. As is already mentioned in literature by Murray (2008a), the citric acid seems to alter the freezing behaviour of water in a way that Cubic Ice I_c seems to crystallize at higher citric acid concentrations at the expense of the hexagonal ice phase Ice I_h . At very high concentrations the droplets do not crystallize any more and stay amorphous. This is insofar interesting as it was not expected that the cubic Ice I_c can form under atmospheric conditions. Even though the citric acid does not occur in the atmosphere in a relevant amount, predictions for the influence of other carboxylic acids can be derived from the gained results.

For the building mechanism of Polar Stratospheric Clouds the nitric acid hydrates play an important role. However, the exact mechanism is not solved yet, and it is also discussed if more hydrate phases do exist, as are mentioned in the literature. Due to the interest on this topic much information on the hydrates already exists in literature, as they were the subject of research by various scientists. For this work, a consequent continuation of the research on the nitric acid hydrates was done, as permission was granted to perform Inelastic Neutron Scattering experiments at the Rutherford Appleton Laboratory in Great Britain. This method is especially sensitive for compounds with a great amount of hydrogen in their structure. Spectra of the nitric acid monohydrate (NAM) and the two states of the nitric acid trihydrate ($\alpha + \beta - NAT$) could be recorded. Through this the state diagram of the trihydrate was proved correct, and new bands could be found for both hydrates. Furthermore, a method was invented for producing amorphous samples of the hydrates in order to gain access to their metastable states.

Acknowledgements

I would like to thank the following people who have supported this work directly or indirectly:

Prof. Hinrich Grothe for the opportunity to work on this topic, for the patient support, and for always being open-minded to new ideas.

Johannes Frank the technician of the Institute of Materials Chemistry for building the Raman cell and for his various good suggestions when it came to experimental procedures.

Karin Whitmore from the University Service Center for Transmission Electron Microscopy of the TU Wien for her supervision of the ESEM measurements.

Rainald Rosner the electronic technician of the Institute of Materials Chemistry for his help with the electronics of the Raman cell.

Dr. Stewart F. Parker from the TOSCA experiment at the ISIS Rutherford Appleton Laboratory in Great Britain for his kind supervision during the experiment, even at night.

The ISIS Rutherford Appleton Laboratory for the granted beamtime, accommodation and the substantial allowance during my stay.

Prof. Thomas Lörting and his group from the University of Innsbruck for the opportunity to carry out the low temperature XRD measurements at their Institute.

Dr. Erich Halwax from the CTA TU Wien for his help with the Rietveld refinements.

Dr^a. Beatriz Martín-Llorente from the CSIC Madrid for the calculations of the NAM spectra.

My family, who always supports me and who gave me the freedom and security to do what I enjoy.

Contents

1	Introduction	1
1.1	General	1
1.1.1	The Climate	1
1.1.2	The Cultural Impact of Climate	1
1.2	Ice Clouds	2
1.2.1	The Atmosphere	2
1.2.2	Cirrus Clouds	5
1.2.3	Polar Stratospheric Clouds	7
1.2.4	Nucleation Processes	8
1.2.5	Different Structures of Solid Water	9
1.3	Radiation Balance	10
1.3.1	General	10
1.3.2	The difficulties of aerosol and cloud analysis	12
1.4	Laboratory Models	13
1.4.1	General	13
1.4.2	Cloud Chamber	14
1.4.3	Aerosol Flow Tube	15
1.4.4	Particle Trap	16
1.4.5	Macroscopic Samples	16
1.4.6	UHV Methods	17
1.5	Motivation	17
1.5.1	Organic Acids in Cirrus Clouds	17
1.5.2	Nitric Acid Hydrates in PSCs	20
2	Methods	22
2.1	General	22
2.2	Model Systems	22
2.2.1	Emulsions	22
2.2.2	Preparation of Amorphous Sample	23
2.3	X-Ray Diffraction	26
2.3.1	Theoretical Background	26
2.3.2	Experimental Setup	28
2.4	Raman Spectroscopy	29

2.4.1	Theoretical Background	29
2.4.2	Experimental Setup	31
2.4.3	Experimental Procedure	32
2.5	ESEM	34
2.5.1	Theoretical Background	34
2.5.2	Experimental Setup	37
2.6	Inelastic Neutron Scattering	38
2.6.1	Theoretical Background	38
2.6.2	Experimental Setup	41
2.6.3	Experimental Procedure	41
3	Results	43
3.1	X-Ray Diffraction	43
3.1.1	Diffraction patterns	43
3.1.2	Rietveld Analysis	45
3.2	Raman Spectroscopy	46
3.2.1	Difficulties and Limits	46
3.2.2	Raman spectra	48
3.3	ESEM	51
3.3.1	10,8 wt% Citric Acid in Water	51
3.3.2	40,4 wt% Citric Acid in Water	53
3.3.3	49,2wt % Citric Acid in Water	55
3.3.4	54,4 wt% Citric Acid in Water	56
3.3.5	59,2 wt% Citric Acid in Water	57
3.4	Inelastic Neutron Scattering	57
3.4.1	NAM	58
3.4.2	NAT	62
4	Discussion	64
4.1	Cirrus Cloud Models	64
4.1.1	Does Citric Acid Suppress the Nucleation of Ice?	64
4.1.2	How does Citric Acid Influence the Phase Composition in General?	65
4.1.3	If Nucleation Occurs How Does Citric Acid Affect the Crystal Growth?	66
4.1.4	Is the Morphology of the Sample Influenced by Citric Acid?	66
4.1.5	What Helpful Spectroscopic Information Can Be Extracted for a Better Understanding on the Molecular Level?	67
4.1.6	Conclusions	67
4.2	INS on Nitric Acid Hydrates	68
4.2.1	The INS Spectra of NAM	68
4.2.2	The INS Spectra of NAT	68
4.2.3	Preparation Method	69
4.3	Outlook	69

Bibliography

71

List of Figures

1.1	Layers of the Atmosphere	4
1.2	Cloud altitudes	5
1.3	Cirrus Clouds	6
1.4	Polar Stratospheric Clouds	7
1.5	Formation of Polar Stratospheric Clouds	8
1.6	Radiation Fluxes	12
1.7	Radiative Forcing	13
1.8	Different models for aerosol investigations	15
1.9	Supersaturation of clouds	18
1.10	State diagram of nitric acid hydrates	20
2.1	Preparation scheme for amorphous samples	25
2.2	Diffraction on solid matter	27
2.3	Raman bands of a silicon waver	30
2.4	Jablonski diagram	31
2.5	Construction plot of the Raman cell	32
2.6	Photo of the Raman cell with and without cover lid	32
2.7	Scheme of a Raman sample	33
2.8	Wehnelt cylinder around a tungsten filament.	35
2.9	The interaction volume of incident electrons.	36
2.10	The ISIS Rutherford Appleton Laboratory in Great Britain	40
2.11	The INS sample holder rod	41
3.1	XRD results for the emulsions at 190K	44
3.2	Calculated crystallite sizes for Ice I_h	46
3.3	Light microscope image of the 49,2 wt% CA emulsion	47
3.4	Different error sources for the Raman experiment	48
3.5	The Raman spectrum of water and of Ice I_h	49
3.6	The Raman spectrum of the samples in the higher frequency region.	49
3.7	The Raman spectrum of the samples in the lower frequency region.	50
3.8	Water evaporation in the emulsion with 10,8wt% CA	51
3.9	The emulsion with 10,8 wt%CA observed under the ESEM	52
3.10	Annealing of the 40,4 wt%CA sample in the ESEM	54

3.11	ESEM image of the 49,2 wt% CA sample	55
3.12	Annealing of the sample with 54,4 wt% CA	56
3.13	Annealing of the sample with 59,2 wt% CA	57
3.14	NAM evolving from an amorphous phase of 50 mol% nitric acid through annealing.	58
3.15	Comparison of different vibrational spectra of NAM	59
3.16	Spectrum of NAM taken at 20K after annealing to 180K.	60
3.17	INS spectrum of α -NAT and β -NAT evolving from an amorphous phase due to annealing.	63
4.1	XRD and ESEM data of selected samples	65
4.2	NAM structure generated from XRD-data.	68
4.3	Falsecolor image of a beautiful hexagonal ice crystal observed with ESEM.	70

List of Tables

3.1	INS bands of NAM in the low frequency range	61
3.2	INS bands of NAM in the frequency region up to 2000cm^{-1}	62

List of Abbreviations

CA	Citric Acid
e.g.	exempli gratia (latin)
ESEM	Environmental Scanning Electron Microscopy
FTIR	Fourier Transformed Infrared Spectroscopy
i.e.	id est (latin)
Ice I_c	Cubic Modification of Ice I
Ice I_h	Hexagonal Modification of Ice I
INS	Inelastic Neutron Scattering
IPCC	International Panel on Climate Change
IR	Infrared
K	Kelvin
NAM	Nitric Acid Monohydrate
NAT	Nitric Acid Trihydrate
PSC	Polar Stratospheric Cloud
SEM	Scanning Electron Microscopy
UHV	Ultra High Vacuum
UV	Ultraviolet
wt%	mass/weight percent
XRD	X-Ray Diffraction

Chapter 1

Introduction

1.1 General

1.1.1 The Climate

The climate on our planet influences life in a strong way. All creatures and plants depend upon certain stable conditions in order to live. Some species have developed through evolution to be able to live even in extreme environments but they still need their special environments and would not prosper fully, or would even perish under drastically changed conditions. The human race is spread over nearly all parts of the planet and is able to live even under uncomfortable environmental conditions by using its intellect and flexibility. But even humans cannot live totally independent of external factors. Therefore stable conditions are necessary for mankind as well. One of the major reasons why earth provides comfortable conditions for its species is the earth's atmosphere. But how does the atmosphere regulate the climate system? Some of the reactions and their effects that take place in the atmosphere are known and understood, but they are outnumbered by the unknown ones. As the climate system is in the focus of interest nowadays due to the temperature irregularities observed over the last decades, it is necessary to investigate atmospheric processes and thus contribute to the understanding of the climate system.

1.1.2 The Cultural Impact of Climate

People have observed the weather and its changes since ancient times. Back then the weather was even more important for the livelihood of ancient civilizations. Food was scarce and the dependence on good harvests was great. Thus the impact of weather or climate changes on the development and culture of human societies was enormous. Very often adverse climatic events were followed by starvation, diseases and sometimes even by migration of the affected people to other places. Due to this fact weather observation was an important cultural issue. People searched for repeating patterns of weather events and tried to use them to their advantage. Very often this knowledge

was linked with sacral ceremonies and worship of deities. Today we search for these patterns as well. Nowadays we can gather information on a higher level, which enables us to gain an even more extensive picture of climate events. With the gathering of more precise information people also developed theories about how certain events such as volcanic eruptions are linked with the climate. Soon the question arose as to how mankind affects the climate and the weather by its own activities.

In 1824 Jean Baptiste Joseph Fourier proposed the theory that gases in the atmosphere contribute to the warming of a planet ¹. With this idea he set one of the milestones for atmosphere and climate research in our time. In 1896 the Swedish scientist Svante Arrhenius published the idea that a change in the amount of CO₂ in the atmosphere may lead to a change in temperature. He predicted that the increasing amount of CO₂ that went into the atmosphere through burning of fossil fuels and other processes can increase the earth's temperature and will prevent the earth from declining into the next ice age ². This idea was discussed controversially in the scientific community at that time. Since then more information was found and his calculations proved to be wrong, as ice ages are linked to other mechanisms as well. But the fact that CO₂ is a relevant IR- absorber and therefore alters the atmosphere is accepted today as a given fact.

In 1988 the International Panel on Climate Change (IPCC) was founded, and since then it collects relevant data on the topic of climate change from scientists all over the world. Along with other information, analysis of the data revealed that over the last decades the overall temperature on the earth was rising. It is still questioned why this happens and what kind of processes are linked to this worldwide event. As the climate is a very complex system it is not only one parameter that needs to be observed and understood. Among many areas that need further investigation are the clouds and how they contribute to the temperature and weather regulation of the earth. Many different cloud types exist which behave differently and may have various effects on the climate. This work focuses particularly on ice clouds and how they could affect the climate.

1.2 Ice Clouds

1.2.1 The Atmosphere

The earth's atmosphere is made up of different gases that are held in place by the gravity field of the planet. Primarily it is composed of nitrogen N₂(78%), oxygen O₂(21%) and Ar(0,9%). Water vapour is a very important component as well, and its

¹Fourier (1824)

²Arrhenius (1896)

concentration varies strongly within the atmosphere. Its concentration can reach up to 3% and is controlled by evaporation and precipitation. The trace gases make less than 0,1% of the atmosphere but their effect is high³. Briefly mentioned, some are able to influence the building of clouds in a very efficient way, while others are strong IR-absorbers and therefore contribute to the so-called greenhouse effect. However, the list of trace gases is long and will not be a subject of further discussion here. Mainly the atmosphere can be divided into five different layers reaching from the surface up to an altitude of around 100 kilometres. With the barometric formula the mass distribution in the atmosphere can be described. The formula explains that the density of the atmosphere decreases exponentially with greater altitude leading to the situation that most of the atmosphere's mass ($\approx 74\%$) can be found in the lower troposphere. Even though this barometric formula is simplified and is only exact for isothermic systems it shows the trend how the atmosphere's mass is distributed.

$$p(h_x) = p(h_0) \exp \left[\frac{-\Delta h}{\left(\frac{RT}{Mg}\right)} \right] \quad (1.1)$$

$p(h_x)$: pressure at an altitude x [Pa]

$p(h_0)$: pressure at sea level 101300 [Pa]

Δh : height difference between h_0 and h_x [m]

R : universal gas constant 8.314 [$\frac{J}{Kmol}$]

T : temperature is assumed constant at 15 [°C]

M : mean molar mass of the atmospheric gases 0.02896 [$\frac{kg}{mol}$]

g : gravitational acceleration 9.80665 [$\frac{m}{s^2}$]

Troposphere Starting from the earth's surface the first layer is the troposphere, which is limited by the tropopause. On the equator the troposphere reaches up to 17 000 metres, and on the poles it reaches up to 7000 metres. The troposphere gains most of its temperature from black body emission of the earth, so the warmest place is the lowest part (where most black body radiation is absorbed) and the temperature decreases with the altitude down to around 205K. As hot air tends to ascend this process leads to a mixing of the air masses and to transport and exchange of air masses in the troposphere. This creates an important part of the weather system. As the troposphere is the layer nearest to the earth it is also the layer with the highest

³Seinfeld and Pandis (1998)

density, and due to this it contains around 80% of the atmosphere's mass. Also, most of the clouds are situated in the troposphere. The tropopause ends the troposphere and is characterised by a sharp change in the temperature trend. The tropopause separates the turbulent troposphere from the stable stratosphere.

Stratosphere In contrast to the troposphere the stratosphere is very calm and low of turbulence. It extends from the tropopause up to an altitude of around 51 kilometres. The temperature in the stratosphere increases with height, which suppresses vertical mixing of the air masses. This so-called convection barrier leads to very stable conditions where the mixing of the air parcels occurs almost solely through diffusion. Through this, the depletion of compounds that reach the stratosphere happens very slowly. As the ozone layer is situated in the stratosphere it is clear why ozone destroying compounds like the Chlorofluorocarbons(CFCs) have such a long time impact on the ozone layer.

The stratosphere is almost free of clouds except for the existence of Polar Stratospheric Clouds near the poles. The stratopause ends the stratosphere and is marked by a change in the temperature development.

Mesosphere From the stratopause up to an altitude of 80 - 85 kilometres the mesosphere is located. The temperature here decreases with altitude down to the temperature minimum that exists on, or more around, the earth where it has an average temperature of 173K. Similar to the troposphere, rapid vertical mixing of air masses occurs due to the temperature scheme where the lower air masses are hotter than the higher ones. The mesopause limits the mesosphere by another sharp cut in the temperature scheme.

Thermosphere The temperature in the thermosphere increases with height until reaching the thermopause, where it stays constant. On average the temperature can rise up to 1770K, but the molecules in the thermosphere are so far apart that temperature is not well de-

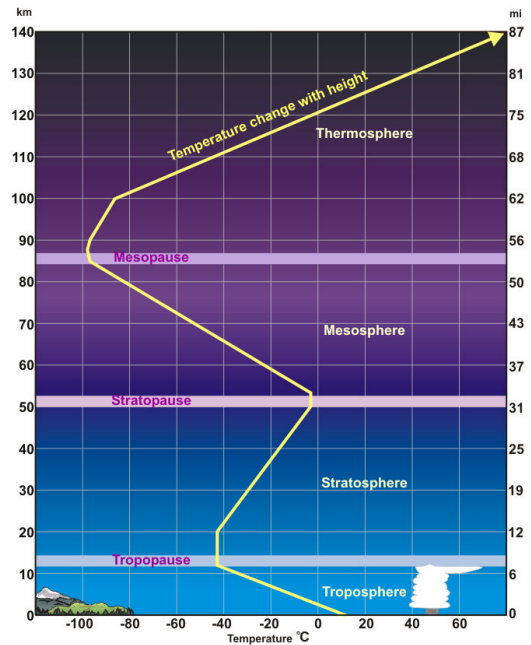


Figure 1.1: Profile of atmospheric layers and their temperatures. Taken from the NOAA

fined there. The Kármán line ⁴ lies in the thermosphere, which is considered as the boundary between the earth and space at an altitude of 100 kilometres. The high temperatures in the thermosphere are a result of short wavelength radiation absorption of N₂ and O₂. Depending on solar activity the thermosphere ends between an altitude of 350 - 800 kilometres.

Exosphere Mainly composed of hydrogen and helium the exosphere is the outermost layer of earth's atmosphere. Here the molecules are very far apart from each other and collide very seldom. Those molecules which have enough kinetic energy can escape earth's gravity field from here into space.

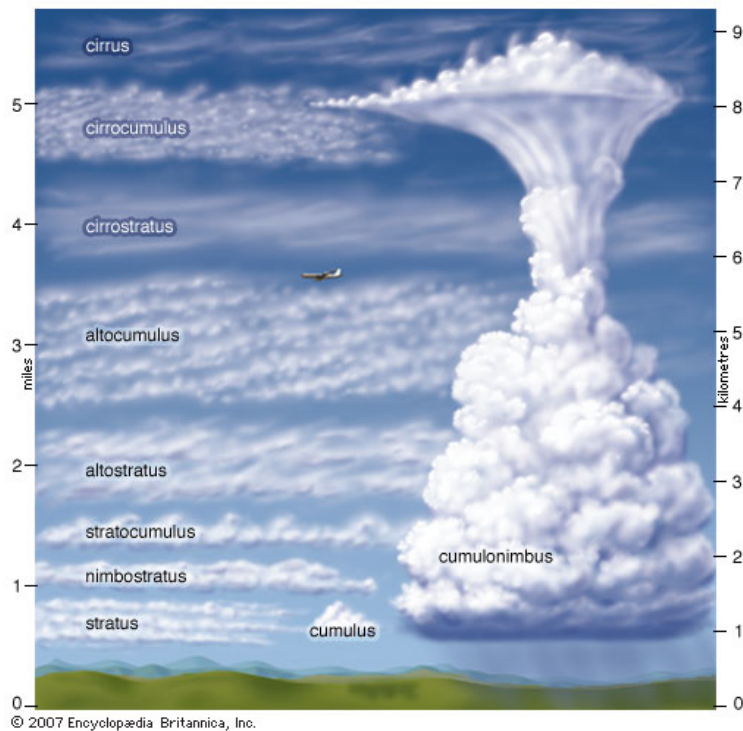


Figure 1.2: Typical altitudes at which common clouds occur. Taken from Encyclopædia Britannica.Inc

1.2.2 Cirrus Clouds

Cirrus clouds are probably the most well known ice clouds. They are easily recognised for their thin and featherlike appearance and can be observed all over the earth with

⁴The Kármán line is an imaginary line at 100 kilometres of altitude. It is named after Theodore Kármán and is commonly used to roughly define the boundary between the atmosphere and outer space. The term is mainly used in aeronautics, as Kármán calculated that an aircraft at this altitude would have to fly faster than earth rotation to gain sufficient ascending force from the atmosphere.



Figure 1.3: Cirrus Clouds

an increased occurrence at the equatorial zones. The clouds exist at altitudes of 8 to 12 kilometres, which is in the upper troposphere. The temperature in these heights is between -30 and -60°C . When ascending air masses rise into these altitudes they cool down and the water vapour forms small ice crystals leading to cirrus clouds. The moisture content of these air masses is normally very low, as air with higher moisture would have formed clouds much earlier at lower altitudes. Due to the low moisture, the ice clouds have a rather low density, resulting in the familiar thin wisplike structure.

When observed, the cirrus clouds appear in a brighter white than other clouds which normally lie beneath them, as the cirrus are among the highest clouds in the troposphere. This bright white is a result of the low optical density of the clouds and of light scattering on the clouds' ice particles. When the sun has set the cirrus can appear in a spectrum going from yellow through red to gray. While other clouds are already dark grey at this time the cirrus are still illuminated from the sun due to their higher altitude, and thus appear coloured.

Traffic airplanes fly at a similar altitude where cirrus clouds form. Cirrus clouds can even be observed well from the airplanes. During the plane's combustion process water is formed in the turbines, which is then released in the form of hot water vapour. This water vapour is then cooled down quickly, forming ice crystals which lead to small clouds behind the plane. These so-called contrails can be seen easily from the ground and have a very similar composition to cirrus clouds. So even if they are of artificial origin they can be included in the family of cirrus ice clouds. It is also being discussed whether anthropogenic clouds may serve as nuclei for the development of more cirrus clouds as discussed by Baker and Peter (2008). Cirrus clouds play an important role for the climate. On the one hand they reflect radiation from the sun, and therefore serve as a cooling factor. On the other hand they trap IR-Radiation coming from

the earth's surface, and therefore serve as a warming factor. It is not fully solved yet if one factor outweighs the other. Even still unrecognized cloud processes may exist with unknown effects on the temperature.

1.2.3 Polar Stratospheric Clouds



Figure 1.4: Polar Stratospheric Clouds

Polar Stratospheric Clouds (PSCs) are ice clouds that exist in the lower stratosphere. They can be observed only in and near the polar regions. The clouds have a beautiful colourful appearance when seen. Due to their existence at high altitudes they can still be illuminated by the sun when it has already set for the observer on the ground. This is similar to the cirrus clouds but the PSCs are even higher and the colours are much brighter.

Records of PSC observations can be traced back to the 19th century where they have been first observed in Sweden in 1870 as mentioned in Stanford and Davis (1974). Since then, PSCs have been observed only occasionally which led scientists to the conclusion that PSCs must be a rare weather phenomenon. It was not until 1982 when McCormick et al. (1982) showed, with the help of satellite observations, that PSCs are not as rare as it was thought. These observations revealed that PSCs are present in the arctic, and with an even increased occurrence in the antarctic regions during the polar winters. Since this discovery many scientists created models for the building mechanisms of these clouds. The sulfuric acid background aerosols which exist in these altitudes play an important part in the building mechanism. Crutzen and Arnold (1986) and Toon et al. (1986) proposed independently from each other that nitric acid might play an important role in the chemistry of the PSCs. Today it is known that sulfuric acid acts as a nucleation agent and gaseous nitric acid is taken up by these particles when the temperature drops. Finally this ternary mixture freezes into different hydrate phases. The exact building mechanisms are not fully under-

stood yet, and especially the phase diagram of the nitric acid at these temperatures still needs further investigation.

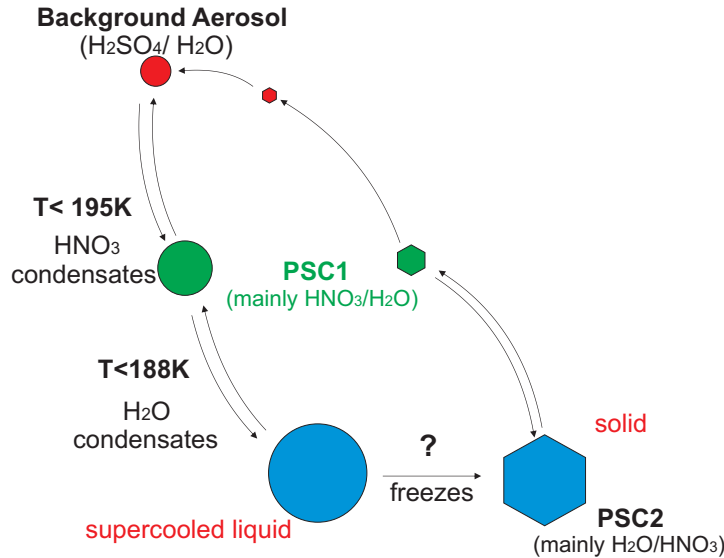


Figure 1.5: Formation of Polar Stratospheric Clouds

PSCs play an important role in chemical chlorine activation and subsequent ozone depletion in the polar stratosphere. Therefore their influence on the ecosystem is high and greater knowledge can lead to a better understanding of this sensitive system.

1.2.4 Nucleation Processes

As this work is going further into detail on the building mechanisms of ice clouds it is essential to define certain terms. For the understanding of ice clouds and how they form, knowledge of ice nucleation in general is useful. If the word nucleation appears in articles concerning clouds or aerosols it must be distinguished between the nucleation event that leads to the formation of liquid droplets and the nucleation event that leads to crystallization of ice particles.

Liquid droplet nucleation forms through supersaturation of water in air masses and occur homogeneously and heterogeneously. Heterogeneously through small dust/aerosol particles where vapour is absorbed and droplets are built around them. Homogeneous nucleation occurs through strong supersaturation of water vapour in the air. This kind of nucleation will not be discussed here further as it does not contribute to the topic of this work. However, it is necessary to know the difference to ice nucleation to avoid confusion.

Ice nucleation describes the freezing mechanisms of liquid water or water in the vapour phase. It is generally known that water freezes below $0^{\circ}\text{C}/273\text{K}$, but what is less known is that the freezing must not start initially at this temperature. Normally if a cup of water is put into the refrigerator it will freeze shortly below zero. But if water is cooled very slowly and is free of particles and very still it can be cooled down to even 70°C below the freezing point. This happens through the fact that freezing starts with an ice crystal germ. Generally there are always accumulations of ordered H_2O molecules in water. These so-called ice embryos decompose as fast as they come together. At -5°C , 50 000 molecules of water need to come together to start a nucleation event which still has a low probability. The amount of molecules that are needed to start nucleation decreases with the temperature. At -20°C it would be just a hundred molecules. Once an ice germ has formed through such a critical mass of molecules it is able to cause the whole mass of subcooled water connected with it to freeze. As the aggregation of the molecules is a stochastic process it becomes clear why large masses of water have a higher probability to freeze at higher temperatures. The chance for the development of a stable germ is therefore directly proportional to the number of water molecules.

The contact of subcooled water with other particles can also induce nucleation and freezing. This is called heterogeneous nucleation. Small dust particles, for example, can act as nuclei for ice in the air, and in agriculture silver iodide is a known agent that is used to cause earlier nucleation and prevent hailstorm. Every other material, may it be of natural or artificial origin, can act as a nucleus. The exact mechanisms as to how the water molecules interact with the solids are complicated, and many compounds that are present in the atmosphere need further analysis. Additionally it has to be said that some compounds may also suppress nucleation, which will be discussed further in section 1.5.

1.2.5 Different Structures of Solid Water

Now brief explanations will be given of some of the solid structures where water is involved. This may serve the gentle reader as a help to avoid later confusion when the expressions appear in the text.

Ice Phases of water are a subject of research that is important for many different areas of science. The common water ice as it is present in winter when the temperature drops below 0°C and the water crystallizes is the hexagonal ice phase often briefly mentioned as Ice I_h . Besides this hexagonal phase, sixteen other ice phases have been identified, forming mostly at different pressures and temperatures. The phase diagram of water ice is not fully solved yet and still holds many interesting questions. Even the discovery of other new ice phases in the future is possible. For investigations in the atmosphere and on the ground most of the ice phases do not play an important role since they form at very high pressures. At atmospheric conditions only hexagonal

ice forms, and just recently it was discovered by Murray et al. (2005) that also the metastable cubic ice phase Ice I_c may form at atmospheric conditions.

Hydrates is the term for all inorganic or organic compounds that are dissolved in water or have water incorporated in their structural formulae. When solid, these hydrates have their own crystal structure different from the crystalline ice phases, from which they are sharply distinguished. The hydrates may have different phases as well with different equivalents of water in their formulae or even different crystalline modification within the same elemental composition. The hydrates of nitric acid will be discussed in this work as they have an impact on atmospheric mechanisms.

Clathrates have in contrast to the hydrates an intact water ice lattice even though they are a mixture of ice and other substances. This comes through the effect that the other molecules that make up the clathrate are caged in the lattice of the water ice, therefore leaving an ice behind which releases these substances when it melts. One prominent representative is the methane clathrate. In its ice lattice, methane molecules are caged which can be released by elevating the temperature over the melting point. This leads to the interesting effect that when ignited, the methane clathrates burn through the released methane.

Amorphous Solids are also known as glasslike solids. Amorphous describes the state where the atoms or molecules do not have any long range order. But also within the amorphous state there can be different states with higher or lower density or different grades of disorder.

The amorphous phase is not always accessible for all compounds. One way to gain access to the amorphous state is by applying very high cooling rates onto a liquid. If this is done the temperature zone is passed in which homogeneous nucleation takes place. However, if the cooling is very fast, the viscosity of the liquid is increasing faster than the propagation of the crystal structure can take place. The high viscosity efficiently suppresses further growth of the crystal structure and a nearly full amorphous solid is gained.

1.3 Radiation Balance

1.3.1 General

One of the major tasks in understanding the complex climate system of our planet would be an accurate knowledge of the radiation balance. According to the report of the IPCC (2007) the radiation balance can be influenced in three different ways:

- Through a change of the incoming solar radiation. This could happen through changes in the earth's orbit or changes in the emitted radiation of the sun. This

is the farthest away from human influence and a change is not expected in a yet relevant timescale.

- Through a change in the radiation fraction that is reflected from the earth. Contributing factors here are the reflectivity of the earth's surface (e.g. reflectivity of soil, plants, snow, or even manmade buildings) and of clouds and aerosol particles in the atmosphere. This is called the albedo, and the influence of mankind as well as the influence of natural events play a role here.
- By altering the blackbody radiation that is emitted from the earth into space. This happens mainly through control of greenhouse gases (GHG), which again is in reach of human influence.

Changes in these three points induce reaction of the climate in direct or indirect ways through various feedback mechanisms. The feedback mechanisms exist in a great variety. Many of the mechanisms are still hidden and unknown to science, but some could already be observed or predicted. There can be positive or negative feedback mechanisms, meaning that they can either amplify the primary event or attenuate it. One example mechanism is the snow melting due to higher temperatures which could expose the darker soil beneath it, leading to lower reflectivity and higher absorption of incoming radiation. This would be an example for a positive feedback mechanism as this would enforce the initial warming.

A different example for a negative feedback mechanism is known for CO₂ and its interaction with plants. The plants need CO₂ for photosynthesis and with the aid of sunlight they turn it into O₂ and higher molecules. With a slightly increased amount of CO₂ in the air the plants are assisted in growing and this in turn lowers the CO₂ amount in the air.

An estimated scheme of the radiation balance was presented in the IPCC report 2007. Looking at this scheme in Figure 1.6 it has to be borne in mind that there are still high uncertainties in many of the drawn fluxes but the scheme helps to imagine the mechanisms well.

As explained before the albedo value is a relevant factor in the radiation balance. What factors contribute to this value and how? The surface of the earth is very important, as well as the reflectance of the clouds and aerosols in the atmosphere. The part that is reflected by clouds and aerosols is larger than the amount that is reflected by the earth's surface, plants and other factors. But the cloud and aerosol reflection holds a high uncertainty. In fact, it was presented as the largest single factor of uncertainty in radiation balance and radiative forcing⁵ according to collected data from the IPCC 2007 as can be seen in Figure 1.7.

⁵If a factor is influencing the climate its impact is often called Radiative Forcing. Radiative Forcing is a measure that describes how a parameter influences the radiation balance. It is called forcing as it describes a move out of the equilibrium of the radiation balance. The unit for the radiation balance is watts per square metre ($\frac{W}{m^2}$)

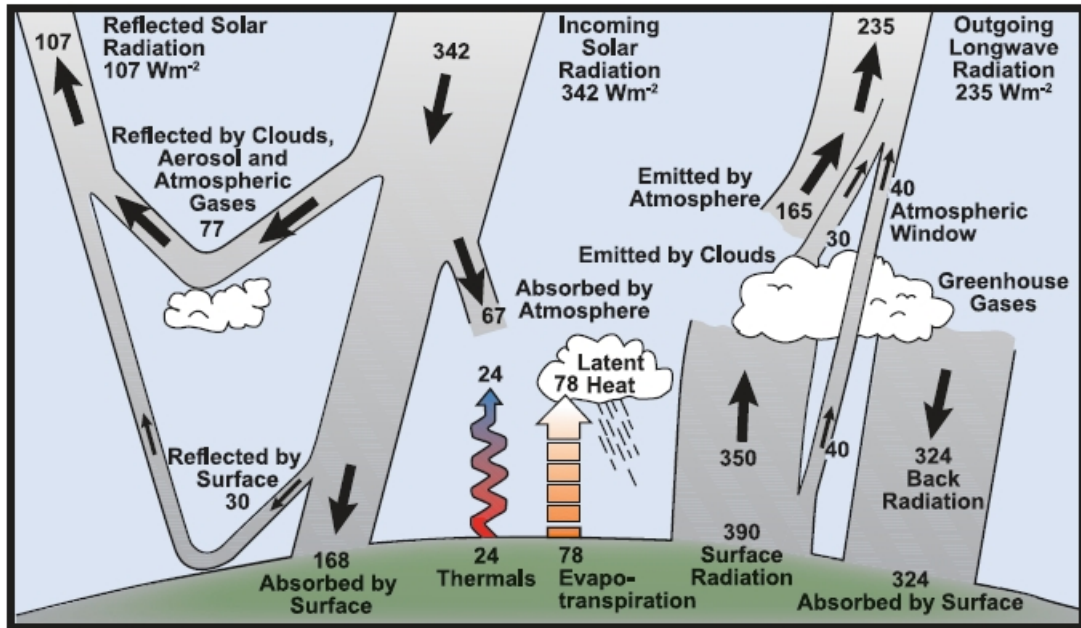


Figure 1.6: Estimated Radiation Flux. Taken from IPCC (2007)

1.3.2 The difficulties of aerosol and cloud analysis

If we look at Figure 1.7 the question arises why the cloud and aerosol fraction holds such high uncertainty. This may be explained by the fact that the reflectivity and sunlight interaction of clouds and aerosols are more complicated to measure and define than for soil or snow surfaces. Why are these important parameters so hard to determine? One factor that can be imagined easily is that the clouds, especially the high altitude clouds, are harder to reach for field measurements than surface material. There are certain methods that can be used to gain data from aerosols and clouds but the expenses are high. The composition of aerosols can be determined by collecting particles with balloons or airplanes and IR data can be gathered by satellites, to name only a few. But especially when it comes to ice clouds the knowledge of the phase composition and the surface information of the particles is very important and can not be determined through field measurements yet. To investigate the phase composition, X-Ray Diffraction measurements have to be carried out that cannot be performed on cloud particles in situ, as the method is limited to a stable setup. The need for laboratory models comes into play at this point which simulate clouds or cloud particles within a stable laboratory, experiment.

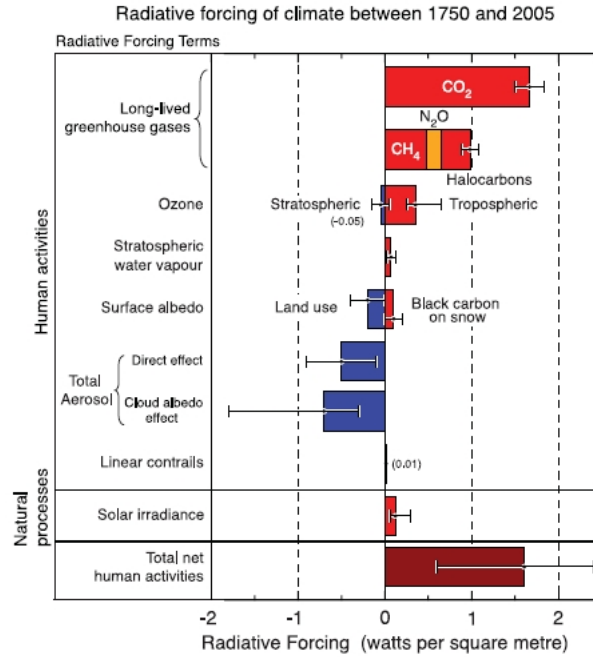


Figure 1.7: Radiative Forcing. From IPCC report (2007)

1.4 Laboratory Models

1.4.1 General

The invention of model systems always comes with the need to determine certain important parameters that are not accessible by field measurements on the real system: But what overall parameters need to be included if one has to characterize clouds? The following points give an overview of the required information.

- Chemical Composition
- Phase Composition
- Morphology
- Surface Structure
- Surface Chemistry

The basic idea is that physicochemical processes, which are not fully accessible in field measurements, can be studied in feasible laboratory models of different dimensions. Figure 1.8 presents this idea as a graphical abstract. Every model exhibits a certain distance to reality, but provides access to particular parameters, which otherwise are inaccessible. With an increasing distance to reality the experimental conditions can be chosen more precisely and the set-up for more sophisticated measurement

techniques is easier to apply. Without doubt, the model next to reality is the aerosol chamber followed by the aerosol flow tube. Both models are large- or medium-scaled pilot plants and contain real aerosols, i.e. an ensemble of particles surrounded by a gas phase. The models next in line already have dimensions suitable for a chemical or physical laboratory; they are termed bench-scale models here. Those bench-scale units focus on the properties of a single particle or the respective simplified model of a particle. Common models in this series are a particle in a levitation trap, a powder or a liquid film in a reaction cell and molecular complexes, clusters and nano-particles investigated by ultra high vacuum techniques. The latter yield only partial aspects of surface structure or nucleation processes, but are indispensable for a precise physico-chemical understanding. In principle, for any strategic approach in the research on extremely complicated systems such a series of scale-downs or scale-ups could be mapped out. However, for the atmospheric systems some particulars have to be taken into account. Temperature and partial pressures of trace gases can change rather suddenly in the atmosphere and most particles are, therefore, not in equilibrium with their environment - the consequence of which are supersaturated gas phases, super-cooled droplets and inherent metastable solid particles. Due to these non-equilibrium conditions, it is rather difficult to find appropriate model substances and to compare findings gathered by different laboratories. Therefore, it is very important to normalize certain results as standards and to file them in data bases. Data collections exist as handbooks, periodicals and review articles (e.g. Seinfeld and Pandis (1998)). Rather often these tabulated values differ for the same component by more than one order of magnitude due to the different approaches in sample preparation and measurement technique. For instance, the uptake coefficient of a certain trace gas on differently prepared ices exhibits remarkable differences. The phase, surface structure, morphology and density of the ices vary strongly with sample preparation. Hence, it is not surprising that an amorphous, porous, low-density ice film prepared by vapour deposition has a much higher capability to take up trace gases than an extended, nonporous hexagonal ice crystallized from a liquid solution. Similar problems exist also for acid hydrates, carbonaceous samples and salt surfaces. However, not only uptake coefficients are affected by the chosen model, but also optical indices, phase composition and chemical composition differ substantially with the model type and the preparation technique. In many cases, the essential physical parameters that vary due to the non-equilibrium conditions are structure, morphology, surface tension, density, viscosity or dissociation equilibria. If, however, a certain problem is monitored by the suitable approach and at the appropriate dimension, it provides the best opportunity to understand the aerosol properties under realistic conditions.

1.4.2 Cloud Chamber

The aerosol chamber is a tank with a large volume, which can be acclimatised and the vapour phase and particle composition can be controlled rather precisely. Therefore the temperature can be varied in a wide array through liquid N₂ cooling in most

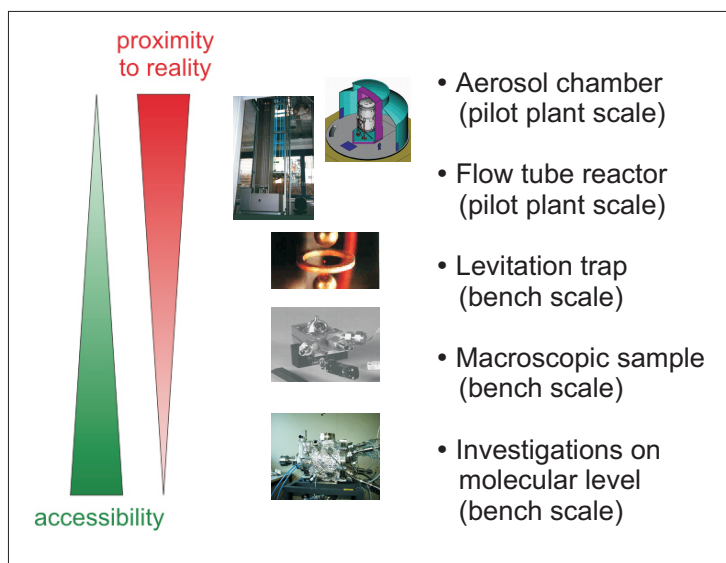


Figure 1.8: Different models for aerosol investigations

chambers. For the production of the aerosols most chambers are also equipped with different devices to produce aerosols and particles. There may be common nozzle nebulizers, ultrasonic nebulizers or carbon spark generators installed to name a few. For the analysis of the particles the chamber is normally equipped with various analytical equipment to determine the particles' parameters such as the size distribution, shape and composition, optical properties and concentrations. From the models for atmospheric aerosols the aerosol chamber is the one that is nearest to reality. But according to Figure 1.8 the access to certain parameters is not possible.

1.4.3 Aerosol Flow Tube

The aerosol flow tube is used for monitoring optical properties, reaction kinetics and uptake of trace gases. Most flow tubes have a minimum detection limit of 108 particles. Thus, an ensemble of particles with a certain distribution of morphologies and compositions exists, from which the optical constants, reaction constant or uptake coefficient can be determined, respectively. However, due to the tube size and the stream velocity the aerosols are affected, showing diffusion, deposition, evaporation, and coagulation, which leads to certain constraints of this method. The confinements of the measurement techniques are the same as for the aerosol chamber. The intrinsic parameters such as phase composition or surface properties are not accessible.

1.4.4 Particle Trap

If single particle properties are wanted, a particle has to be isolated or generated in isolated form. The particle can be levitated in order to be contactless and undisturbed. Levitation (lat. levitas, lightness) is the process by which an object is suspended against gravity, in a stable position, without physical contact. There are three different possibilities how to generate a contact-free particle:

1. optical levitation (Ashkin and Dziedzic (1975))
2. electrodynamic levitation (Paul and Raether (1955))
3. acoustic levitation (Lierke (1996))

Each technique has its assets and drawbacks. Even though the methods are very beautiful, the explanation of them would go too far into detail here, but can be looked up in the literature.

1.4.5 Macroscopic Samples

Macroscopic samples comprehend many different model systems and preparation methods. All of them have in common that the sample size is bigger than one single droplet and small enough to be handled on the laboratory bench. Very often macroscopic samples are handled in some kind of reaction cell to adjust parameters such as pressure and temperature and to keep pollutions away from the sample. For some investigations even thin films of liquids or ice on an inert sample plate can lead to the desired results. Also small capillaries as used by Grothe et al. (2006a) or droplets on hydrophobic coated surfaces have already served as appropriate models. The variety of model systems is great. If certain challenges require new model systems they are designed and brought into form by the imagination of the scientists within the limits of feasibility.

One model system that needs further mentioning here is emulsions. An emulsion exists of two phases that are not soluble into each other. If these phases are mixed thoroughly and long enough a stable emulsion may evolve. This means that the phase with the smaller volume is broken up into small droplets that are surrounded by the other phase. Commonly known examples of emulsions may be milk or the mediterranean Aioli. For research tasks an emulsion can be created with a watery phase and an oily phase. When the watery phase is broken up into droplets through stirring it can serve as a model system that can be handled easily with the advantage of having independent small droplets. As this model system was used to investigate one of the main themes of this work it will be explained more in detail in the coming Chapter 2.

1.4.6 UHV Methods

UHV (Ultra High Vacuum) methods tend to be far removed from traditional atmospheric investigations but go more into fundamental physicochemical research. This does not impair the use and functionality of UHV results for atmospheric science, but it must be clear that this model cannot be compared directly with a real system. But besides this, the experimental parameters can be adjusted very accurately, and therefore sensitive molecule species can be analysed that are hardly accessible through other ways. There are many analytical methods that can be applied on UHV apparatuses. One typical experimental setup would be matrix isolation spectroscopy. For this method an inert gas (mostly argon) is frozen out with a species one wants to analyse with the spectrometer. Commonly, the species that are analysed with this method are very sensitive or short lived molecule species. To preserve the desired species the amount of argon in the gas mixture is chosen much higher so that it is encapsulated in an argon matrix at approximately 6 Kelvin. In this form the molecules can hardly move in the lattice and do not react off, which would have happened immediately under standard conditions. This enables the scientist to apply spectroscopy within possible time scales. Another effect is that in matrix spectra the rotational band broadening is suppressed by the matrix as the molecules cannot rotate within the cage. Through this, sharp bands can be achieved in a matrix spectrum which can be interpreted very well. This is just one of the opportunities that are possible through UHV equipment. The benefit for atmosphere research is great, as with such a system some reactions that take place in the atmosphere can be observed step by step with spectroscopic methods.

1.5 Motivation

1.5.1 Organic Acids in Cirrus Clouds

As mentioned in Section 1.3 the IPCC report 2007 pointed out that there is very high uncertainty regarding the aerosol and cloud impact on the radiation balance. Even though the ability to observe and analyse aerosol particles improved significantly over the last decades, there is still much information lacking. Especially the freezing processes of droplets in the atmosphere still bear many unresolved mechanisms. As freezing strongly affects the properties of a cloud, the understanding of its mechanisms would be desirable. This necessity is underlined by observations in field measurements which could not be explained firsthand by the already known mechanisms. In a paper, Peter et al. (2006) compared data from different field measurements and came to an interesting conclusion. It was concluded that sometimes the nucleation of ice particles does not correspond with the theoretical predictions. Often ice particles seem to show a hindered nucleation or growth, even though all requirements for ice nucleation are present. The summary of different field measurements with airplanes and balloons revealed that there are three major ways in which humid air masses behave when

they are cooled down. Referring to Figure 1.9, the challenging question is now why the lower two events (orange and red lines) take place, as they do not fit into the expected behaviour of water crystallization.

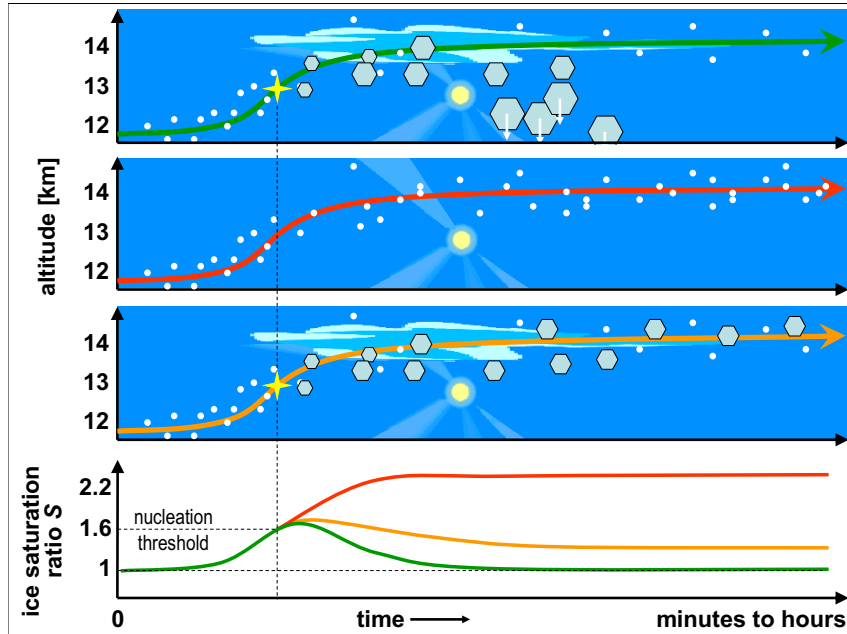


Figure 1.9: Observed nucleation behaviour of upper tropospheric clouds. From Peter et al. (2006)

What circumstances could cause this hindered nucleation? If a closer look is taken at atmospheric aerosols it will be revealed that besides water, there are many different constituents present. This mixture includes acids, salts, and other substances which affect the behaviour of clouds. For many inorganic salts, acids and particles, low temperature experiments have already been carried out. This data is supporting researchers in field experiments very well even though sufficiency can hardly be achieved.

The organic compounds have not been in such a focus of interest yet but their influence may solve some of the anomalous behaviour. There do exist different carboxylic acid mixtures in the atmosphere and there is the need to gather more information about their low temperature behaviour in combination with water ice. As explained in Section 1.4 certain parameters can only be determined in laboratory experiments as yet. So models have to be found which can be used to work with. One very important piece of information when it comes to freezing is the knowledge of the phase composition. This task can be accomplished by doing low temperature diffraction experiments. It was mentioned briefly in Section 1.4 that a stable setup is necessary for diffraction experiments. But how can a diffraction experiment be carried out on a sufficiently large number of droplets to represent a cloud and statistically mean the nucleation temperature?

This problem was solved in a very elegant way by B.J.Murray. The favoured acid/water mixture was stirred with an oil until it became a stable emulsion. In this state the mixture could be cooled down and a Powder Diffractogram could be taken. It was revealed that with an increased amount of citric acid in the water the metastable cubic ice phase increases, and at high concentrations the water does not crystallize during freezing but stays as an amorphous solid, as published in Murray et al. (2005), Murray (2008a). These results are insofar interesting in that it was not thought that cubic ice might be present in relevant dimensions in the atmosphere. That the high concentrations of citric acid in water leads to amorphicity when cooled down could be guessed, as this effect is already known of some salts, acids or carbonaceous materials. But with this information other questions come forth in order to understand this process better and perhaps connect it with the problem of suppressed nucleation or growth.

The upcoming questions are the following:

- Does citric acid suppress the nucleation of ice?
- If nucleation occurs how does citric acid affect the crystal growth?
- How does citric acid influence the phase composition in general?
- Is the morphology of the sample influenced by the citric acid?
- What helpful spectroscopic information can be extracted for a better understanding on the molecular level?

These questions are the basis for this work and for leading to the methods that were applied to achieve these goals.

For the citric acid emulsions the following methods were applied:

- X-Ray Diffraction was carried out to gain information about the phase composition.
- Environmental Scanning Electron Microscopy(ESEM) was used to observe the morphology of the samples.
- Raman Spectroscopy was applied to get a look at the spectroscopic information of the droplets.

The methods and the experimental setup will be explained in detail in Chapter 2

1.5.2 Nitric Acid Hydrates in PSCs

Besides sulfuric acid and water, nitric acid plays a key role for the chemistry of Polar Stratospheric Clouds. As the PSCs are known to play a large part in the mechanisms of ozone depletion, a great deal of research has been carried out already with the aim to understand the building mechanisms of Polar Stratospheric Clouds and their impact on ozone depletion. So the state diagram of the nitric acid hydrates became refined over time and the understanding of the preferred building conditions for the hydrates was also enlarged.

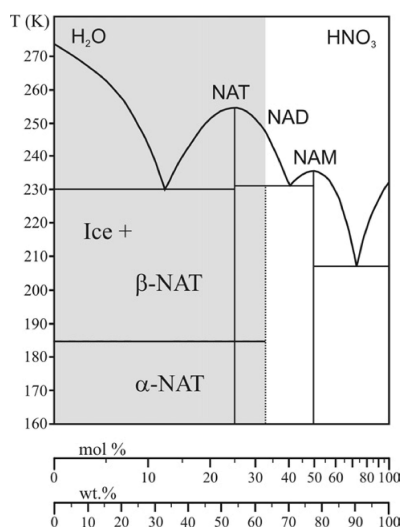


Figure 1.10: State diagram of nitric acid hydrates

The question is, how all this knowledge, mostly gained from laboratory experiments, can be applied to improve the output of field measurements. It was mentioned in Section 1.4 that for a profound investigation of aerosol droplets information about the phase composition is essential. This information is not accessible first hand in field measurements but can be obtained through the connection of the laboratory data with field measurements. Concerning XRD, Raman and IR spectroscopy much published data already exists. This data led to sighting of bands in the spectra that can be used to distinguish between the different phases even in IR and Raman spectra. But not all of these bands are in a spectral range that is accessible for field measurements (which mostly happens through the fact that other compounds in the atmosphere absorb in the same region). So it is especially interesting to find new bands or patterns that can help to distinguish between different phases in atmospheric aerosol and to enlarge the accessible information. Especially the far infrared region is expected to show many

characteristic bands and patterns (fingerprint region). This region has bad accessibility and signal to noise ratio in some spectrometers. One method that besides other advantages shows very good resolution in this region is inelastic neutron scattering (INS). This method is especially sensitive to hydrogen, which makes it very suitable for the nitric acid hydrates. A downside may be that this method needs a reactor source or a particle accelerator so the invitation to such a scientific site is needed. As this opportunity was given, some of the nitric acid hydrates could be analysed with INS.

Among the analysed compounds was also nitric acid of 50wt %, a concentration that has no relevance for the atmosphere and builds the monohydrate of nitric acid. But there is also a good reason to analyse this substance under the topic of atmospheric aerosol research. For research on atmospheric compounds not only the immediate analysis (may it be of spectroscopic, diffractive, elemental, or other nature) of the compound is necessary, but also the need to develop computer models. These models can then generate forecasts for more complex analytical setups of similar compounds. The NAM is interesting for the connection of spectroscopic and theoretical studies. Because its lattice is simple, many simulation models can be used on the NAM, and the models' accuracy can be compared with spectroscopic studies. The refining of these models may lead to a point where more complex structures such as other hydrates might be solved with sufficient accuracy.

Chapter 2

Methods

2.1 General

The used methods refer to the ones that have been mentioned in Section 1.5. For all applied methods, the theory will be covered only very briefly, with only the most important explanations and equations given. This is done due to the fact that the theory about one method may fill a thesis without being sufficient and there already exist very good books that cover these fields. Whenever there may be an extended knowledge of interest or benefit for the gentle reader I will mention some books or articles that cover the field.

On the other hand, the experimental procedures will be explained in detail, as the preparation methods are sometimes tricky and might lead to unwanted results if carried out slightly differently. As this description should enable others to reproduce the experiments, all the details that might influence the sample preparation and the analysis will be given to avoid failure.

2.2 Model Systems

To gain access to certain properties such as thermodynamic metastable phases or independent small droplets, model systems and special ways of preparation had to be used.

2.2.1 Emulsions

For the investigation of citric acid and its influence on the freezing behaviour in small droplets the idea of using emulsions was taken up. This kind of model system was already used by other scientists as Murray et al. (2005), and proved to show very acceptable behaviour.

What are the certain advantages of emulsions over the same amount of the pure liquid (e.g. a watery citric acid solution)? As the freezing process, or in detail the

nucleation, is a stochastic process as explained under Section 1.2.4, using the pure liquid shows some disadvantages. When a liquid system of some ml is cooled down the development of one crystal seed will cause the whole system to crystallize even if the rest of the liquid has no nuclei yet. Therefore the freezing temperature of such a sample always lies higher than for the same amount of liquid if present as aerosol droplets. The emulsions proved to simulate the aerosol pretty well in this point, as the crystal information cannot propagate through the oil matrix. Therefore it is like having an aerosol but with the good handling properties of a solution.

The preparation of the emulsions pretty much followed the explanation given in the paper Murray (2008a). Therefore, 10% of lanoline were dissolved in mineral paraffin oil at a temperature of 40°C with a magnetic stirrer. Then the aqueous citric acid solution was mixed with the oil phase in a ratio of 40/60; water/oil. In this stage the two phases were still separated, but after stirring the solution for one hour with the magnetic stirrer the aqueous solution was fully emulsified in the oil. This happens as the lanoline acts as the surfactant between the two phases. After this process the emulsion is very stable and phase separation does not set in even after months. It does show sedimentation after some time, but only a quick stir or shake is needed to disperse the droplets again.

Six different samples were prepared with the same concentrations of citric acid in water as was used by Murray (2008a) to have comparable results. The prepared emulsions were the following:

1. pure water
2. 10,8 wt% citric acid in water
3. 40,4 wt% citric acid in water
4. 49,2 wt% citric acid in water
5. 54,4 wt% citric acid in water
6. 59,2 wt% citric acid in water

2.2.2 Preparation of Amorphous Sample

The investigation of nitric acid hydrates is insofar challenging as the access to metastable phases is not always easy. It is problematic, because a metastable phase cannot be prepared by just cooling down the sample, as the stable phases build primarily and they do not disappear or change into metastable phases once existent. In the past this problem was solved by preparing amorphous films on a cold surface and subsequent annealing. This worked well and also followed the predictions of the *Ostwalds Step*

*Rule*¹. The problem with this preparation method was that the amount of sample was limited to thin films. For the investigations that had to be carried out for this work larger amounts were needed. To achieve this the preparation method was adjusted to produce several grams of the amorphous sample. The invented method is simple and easy to reproduce. A nebulizer of Meinhard[®] which produces aerosol of several μm was adjusted very close above a dewar containing liquid nitrogen. An aluminium funnel was placed into the dewar to collect the material and to guide it into a sample container that lay on the bottom of the dewar. As the droplets are very small the cooling rate is extremely high, which increases the chance to produce amorphous material. This method proved to produce an amorphous sample of the nitric acid hydrates with a good reliability.

¹This effect proposed by William Ostwald is a rule-of-thumb stating that from an amorphous phase the energetically most favourable state will not always form, but rather metastable phases which are energetically nearer to the amorphous/liquid state.

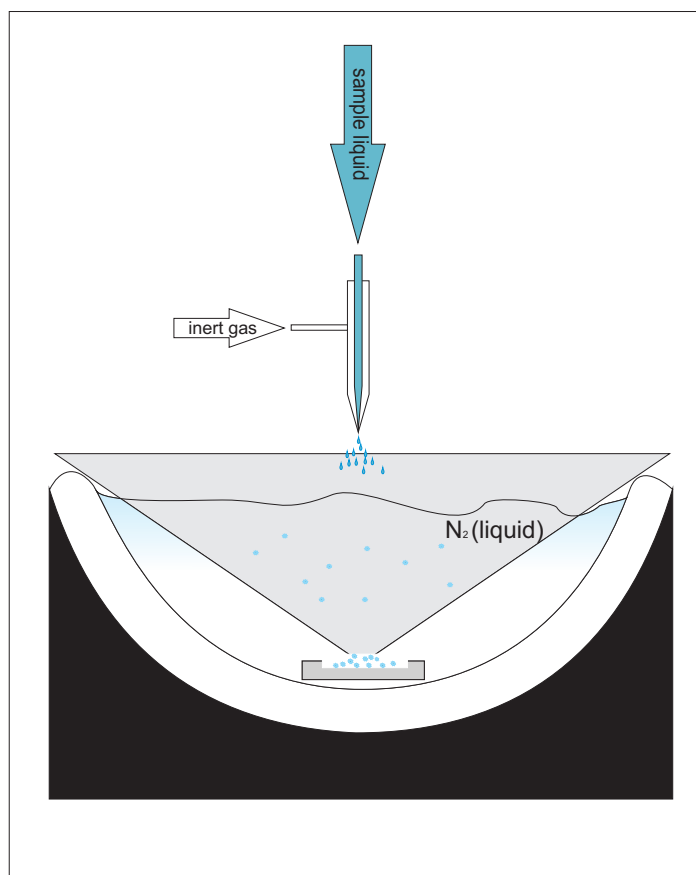


Figure 2.1: Preparation scheme for amorphous samples

2.3 X-Ray Diffraction

To determine phase compositions X-Ray Diffraction(XRD) is the state of the art method. For this experiment the XRD measurements of Murray (2008a) were reproduced with the aim to see if the used model system shows the same properties and if so, to reproduce the measurements with an increased resolution. The better resolution should enable one to calculate the crystallite sizes.

2.3.1 Theoretical Background

Diffraction signifies an effect that occurs when an electromagnetic wave encounters an obstacle. It describes the bending of waves around small obstacles and the spreading of waves out of small openings. Behind the obstacle the wave (e.g. laserlight) shows a characteristic pattern. Under certain fixed and known parameters this pattern can then aid to gain information about the obstacle that caused the diffraction.

The matter now consists of atoms or molecules that are arranged in a system which repeats periodically. This periodic pattern can act as a grid on the atomic scale causing diffraction for X-rays, as their wavelength is partly in the range of atomic distances. These attributes can be used to reveal information of the crystal lattice on which diffraction took place.

For the description and the calculations the system is simplified without causing great errors. Therefore the atoms in the crystal are thought of as plain parallel layers. A crystal consists of a multiplicity of these parallel layers. If the X-rays are diffracted on these crystal planes their diffraction waves interfere. The highest intensity shows when the path differences between the waves of the neighbouring crystal plains are integer multiples of the wavelength λ (i.e. constructive interference).

This correlation is described by *Bragg's law*, which is fundamental for XRD and refers to the variables in Figure 2.2.

$$n\lambda = 2d\sin\Theta \tag{2.1}$$

n : rank of diffraction [usually 1]

λ : wavelength [\AA]

d : distance between crystal planes [m]

Θ : angle between incoming ray and crystal surface [$^\circ$]

When a standard diffraction experiment is carried out the operator gains data of Θ . As the wavelength λ and the rank is known the distance d can be calculated. The distance d between the crystal planes is characteristic for a crystal, so the diffractogram holds a great deal of specific information as to the phase composition.

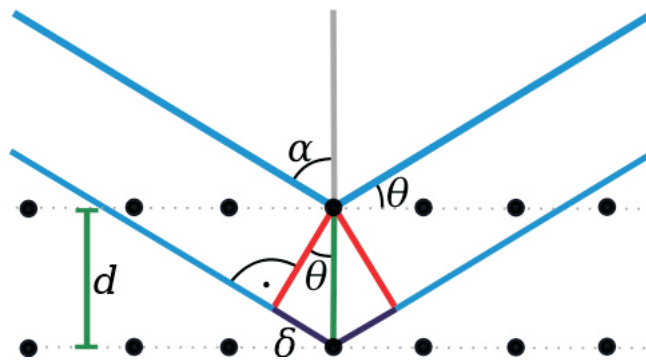


Figure 2.2: Diffraction on solid matter

Other important information that can be extracted from a diffractogram is the size of the crystallites $D[\text{\AA}]$. This can be done as the half-width of the reflexes in a diffractogram is proportional to the size of the crystallites. This connection is expressed in the *Debye-Scherrer-Formula*.

$$D = \frac{K\lambda}{(\Delta 2\Theta)_{cryst} \cos\Theta} \quad (2.2)$$

K : geometric correction factor depending
on the shape of the crystallites

λ : wavelength of x-rays[\AA]

$\Delta(2\Theta)$: half-width[$^\circ$]

Another more sophisticated way to get information about crystallite sizes is by performing a Rietveld refinement. This is a computer based calculation which besides other parameters also calculates the crystallite size. For the Rietveld refinement many parameters of the crystal phases, and also of the equipment, must be known and given beforehand as they contribute to the result.

Further information on Powder XRD can be found e.g. in Jenkins and Snyder (1996).

2.3.2 Experimental Setup

The citric acid emulsions were analysed in a powder diffractometer (Siemens D5000) in theta/theta geometry. For the analysis all samples mentioned in Section 2.2.1 were analysed. As the crystal phases were the focus of interest the samples needed cooling down to 200K. This was achieved by using an evacuable cooling chamber from Anton-Paar (TTK450). The cooling in the chamber was performed with a liquid nitrogen system and the exact temperature was adjusted with a small heating element.

For the analysis a small amount of sample ($\approx 0,5ml$) was given into the depression of the clean sample carrier. Then the cooling chamber was closed and evacuated to 10^{-1} mbar without any cooling yet. One problem that was encountered during this process was that the sample used to outgas very slightly. This sometimes led to bubbles that stayed on the sample surface. They could be erased through venting and reevacuating of the chamber. Then the sample was cooled down to 200K with a cooling rate of approximately 2K/s. At 200K the temperature was held for 15 minutes before measuring to ensure temperature stability. During the measurement the temperature stayed constant within a $\pm 2K$ range. The range of measurement was from 10 to $54^\circ 2\Theta$ and Copper $K\alpha$ radiation was used.

2.4 Raman Spectroscopy

Raman spectroscopy was used to see if during the freezing process of the emulsions differences within the droplet can be made out and distinguished by their spectroscopic data. For this task a cooling chamber for the Raman spectrometer was designed to cool the samples down to 220K. Then all samples were analysed at three different temperatures.

2.4.1 Theoretical Background

The Raman effect that builds the basis for Raman spectroscopy was first mentioned in 1923 by A.Smekal, who made the prediction that this effect must exist. In 1928 the Indian physicist C.V.Raman proved this experimentally. Similar to IR-spectroscopy the transition between different vibrational energy levels builds the basis for the Raman effect although the mechanism is different from IR-spectroscopy. For Raman spectroscopy strong sources of monochromatic light are needed. This led to the situation that Raman spectrometers were not invented until the development of capable lasers many years after the discovery of the Raman effect.

For Raman spectroscopy a sample is illuminated with a strong laser and thus producing spectroscopic information. If the laser light radiates onto a sample most of the light goes through the sample without interference and only a very small amount of the incident light is scattered by the material. The biggest part of the scattered light has the same wavelength as the laser light source. This light is caused by elastic scattered light which is called Rayleigh scattered light. The smaller amount ($\approx 10^{-7}$) is inelastic scattered light which is called Raman-scattered and has different wavelengths than the laser light source. From the wavelength shift of the Raman-scattered light it is possible to gain information about the material. The shifted bands always appear symmetrically around the Rayleigh band situated at the wavelength of the incident light. To every Raman band i there exists a band in the low frequency range (lower than the Rayleigh band) of the spectrum with $\nu = \nu_0 - \nu_i$, and a band in the high frequency part (higher than the Rayleigh band) with $\nu = \nu_0 + \nu_i$. The higher frequencies occur due to so-called anti-Stokes scattering whereas the lower frequencies occur due to Stokes scattering. In the spectrum the bands are specified in wavenumber shifts (cm^{-1}) from the Rayleigh band which defines zero. But as explained, the Rayleigh band has an intensity that is factors higher than the Stokes and Anti-Stokes scattering. To have comparable band sizes the Rayleigh band is always filtered to lessen its high intensity.

Pure silicon is often used to calibrate or adjust the system as it has only a single band. The Si-Si vibrational band is at $520 \pm 2cm^{-1}$. In Figure 2.3 a spectrum of a silicon waver is seen. The Rayleigh band is at zero and the Stokes and Anti-Stokes scattering of Si-Si can be seen very well at $520 cm^{-1}$. Furthermore it can be seen that the Stokes scattering is weaker than the Anti-Stokes scattering.

The mechanisms that lead to these bands will be explained shortly with aid of the

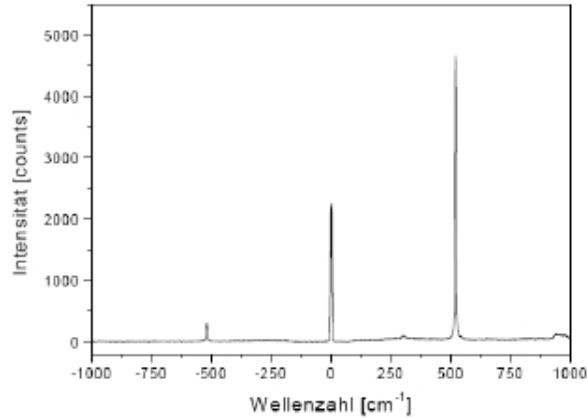


Figure 2.3: Raman bands of a silicon wafer

scheme in Figure 2.4, a so-called Jablonski diagram illustrating the processes nicely. If the incident light falls onto matter a photon with the energy ν_0 is absorbed by the molecule, stimulating its energy level to shift from the ground state to an intermediate electron state with a virtual energy level. The virtual energy level is not a real stable energy state of the system and can lie between the ground state S_0 and the first excited electron state S_1 depending on the frequency of the incident radiation. From this virtual energy state the most likely event is the return to the ground state. If this happens, radiation of the frequency ν_0 is emitted, which is the Rayleigh radiation. With lower chances the electron may also fall back to the first excited vibrational state v_1 . The emitted energy and therefore the frequency is lower and redshifted. This effect causes the Stokes scattering. If the electron is already in the first vibrational state v_1 and is stimulated it may fall back to the ground state after stimulation to the virtual level. In this case the energy that is emitted is higher than the initial incident radiation that was needed to reach the virtual level. Thus the frequency is blueshifted, which is the Anti-Stokes scattering.

The Rayleigh scattering is called elastic as there is no energy exchange from the photon to the matter, whereas the Stokes and Anti-Stokes scattering is called inelastic, as energy is exchanged leaving the matter in a higher or lower energy state.

Similar to IR-spectroscopy there are also certain selection rules for Raman spectroscopy. For a vibration in Raman spectroscopy it is necessary that the polarizability is changed with the vibrational movement to produce bands in the spectrum.

A comprehensive introduction to Raman spectroscopy can be found in Skoog et al. (2006) and further information on confocal Raman spectroscopy can be found in Diening et al. (2011)

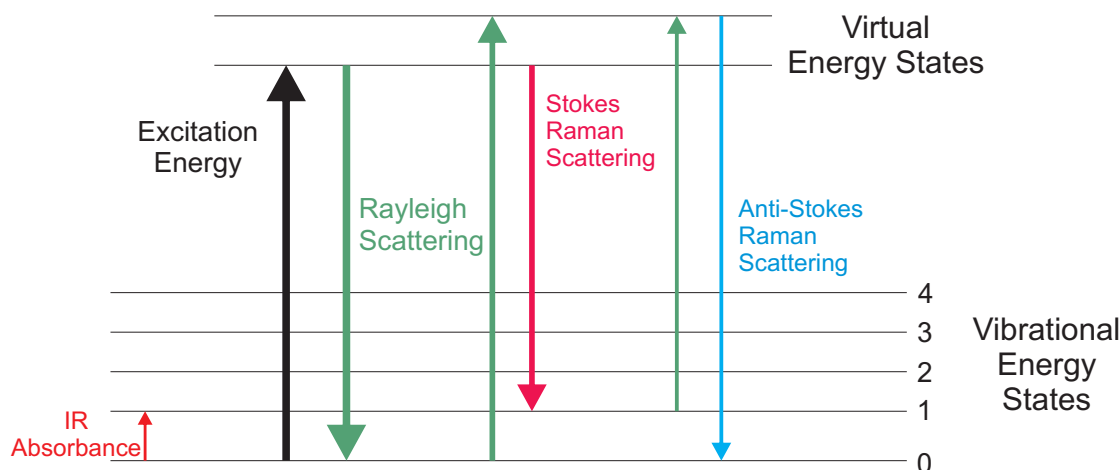


Figure 2.4: Jablonski diagram

2.4.2 Experimental Setup

A Raman Spectrometer with light microscope of HORIBA-JobinYvon was used. The laser was a He-Ne laser with 633nm wavelength and the measurement range was adjusted with an optical grid. The spectrometer was calibrated once a day with a silicon waver by adjusting the Si-Si band at $520 \pm 2, 5 \text{ cm}^{-1}$. The accuracy of the spectrometer in general is within $\pm 2 \text{ cm}^{-1}$.

The task of the measurement was to spot differences in the freezing behaviour of the emulsions. Therefore, cooling of the sample down to upper tropospheric temperatures was needed (i.e. $\approx -60^\circ\text{C}$). To reach these temperatures a cooling cell was built with a three stage Peltier element. On top of the uppermost Peltier element a thin glass plate was placed to keep the ceramic surface of the Peltier element clean against the sample which was placed on the glass plate. Furthermore a temperature-element type-K was fixed on the ceramic surface with temperature conductive glue to observe the temperature over the time. The whole sample cell was built of Teflon[®] and had a copper heat exchanger built in at the bottom to cool the Peltier element. The heat exchanger had a circular flow of ice water to take up the heat from the bottom of the Peltier element. A temperature of -55°C could be reached with this construction.

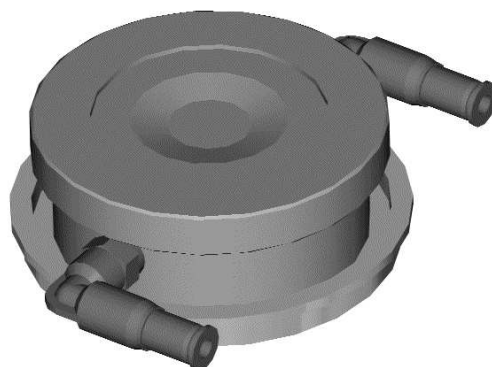


Figure 2.5: Construction plot of the Raman cell

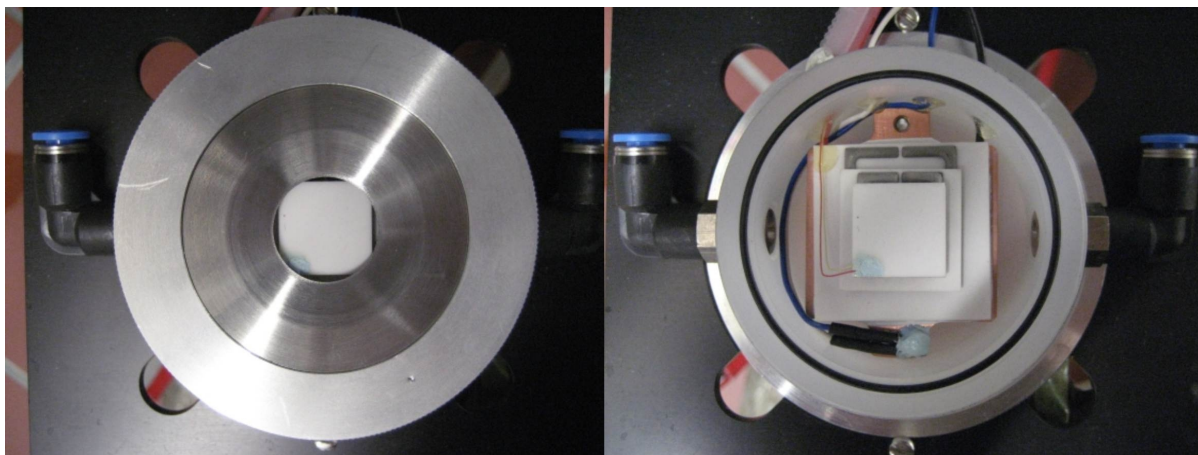


Figure 2.6: Photo of the Raman cell with and without cover lid

The cell was built airtight within its needs and could be flushed with nitrogen gas or any other dry gas to remove humidity from the chamber. This was done to prevent the water vapour from freezing out on the sample surface and on the conductive parts of the Peltier element. To reach the sample with the laser from the Raman spectrometer a thin glass window was built into the cover lid of the cooling cell which can be seen on the left photo of Figure 2.6.

2.4.3 Experimental Procedure

For the experimental procedure a small amount of sample was placed in the sample area of the cell. Then another glass plate was put on the sample resulting in a sandwich construction. This had the benefit that the sample was compressed and was present as a thin layer which made it easier to focus on single droplets with the

microscope. In general the focussing of the laser and the microscope was a little bit challenging as the contrast between the droplets and the oil matrix is not very strong. If this was accomplished a measurement at 14°C was started. Then the sample was cooled to 0°C and measured again and finally to -55°C . The measurement included a Raman spectrogram between 100 and 4000 cm^{-1} once in the middle of the droplet, once outside in the matrix. This was done for all different emulsions. Before a measurement was started the temperature was kept constant for 15 minutes to ensure the same temperature in the whole sample.

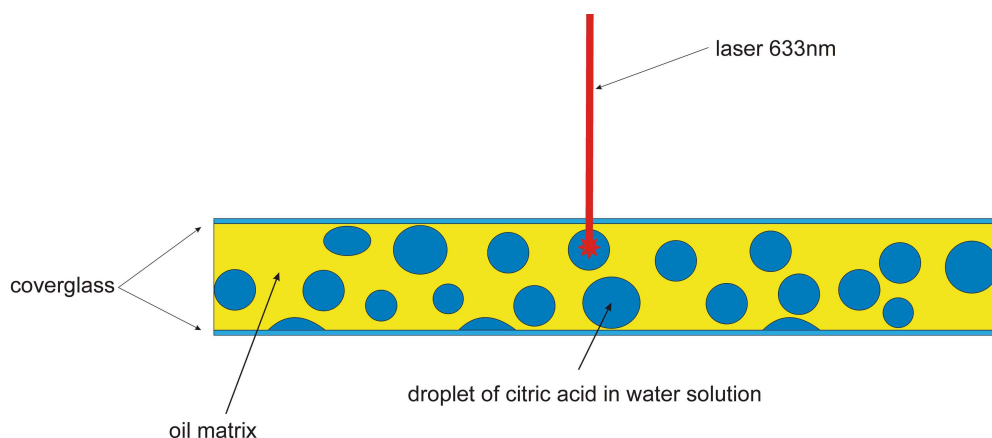


Figure 2.7: Scheme of the sandwich construction, as it was used to place the samples into the cooling cell

2.5 ESEM

Environmental scanning electron microscopy (ESEM) is a special operation mode of a scanning electron microscope (SEM). Standard SEMs work under high vacuum of $\approx 10^{-10}$ mbar to prevent the electron beam from weakening through interaction with gas molecules. ESEMs are able to work efficiently under higher pressure up to (≈ 0.1 mbar). In the ESEM the sample is observed under the pressure of an imaging gas. This enables the scientist to observe samples that would have evaporated under the lower pressures of a standard SEM. Actually, the water ices are among those substances that have been hidden to our view through a SEM, but can now be observed with the ESEM method. ESEM is only one method among many others which can be used to gain information about ices. Even though out of an ESEM picture certain hard facts such as structural or bonding information cannot be extracted, it can be used as a puzzle part together with other methods to result in a better understanding of the ice compounds. For this work the use of ESEM was essential as the high vacuum in a standard SEM would have caused the emulsion samples to evaporate, which could be prevented by working in higher pressure ranges.

2.5.1 Theoretical Background

As ESEM is a special operation mode of a SEM enabled through certain modifications, the image producing mechanisms are generally the same for SEM and ESEM with only little differences. There are different signals that can be collected with a SEM and, depending on what signal is detected, different information is accessible. The signals result from the interaction of a primary electron beam with a sample matter.

Electron Source To produce the electron beam there is the need for an electron source. Different electron sources are available today, all of them with their special benefits and downsides. Common sources are field emission guns or glow filaments of tungsten or LaH₆ Lanthanhexaboride. For the glow filaments materials with a low work function are chosen. The filament is heated and emits electrons during this process. Around the filament there is normally a focusing device called Wehnelt cylinder that serves as the first focus for the electron beam due to its positive charge. The source must always be held under high vacuum (10^{-9} mbar) as the electron beam would diminish instantly under higher pressure.

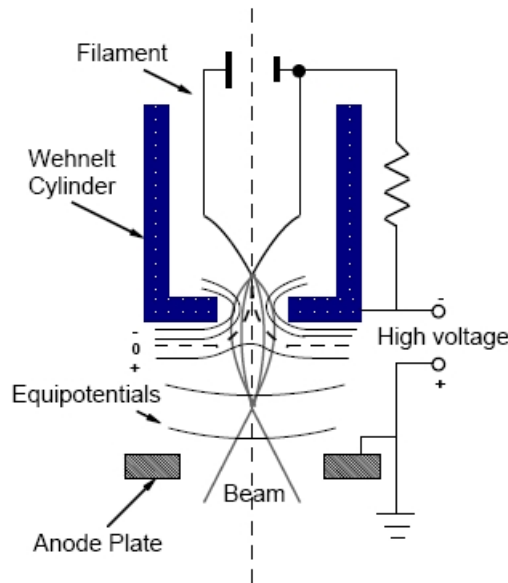


Figure 2.8: Wehnelt cylinder around a tungsten filament. From Waller (2007)

Focusing the Electron Beam The emitted beam from the Wehnelt cylinder is guided through several condenser lenses to achieve the required grade of focus. Condenser lenses are electromagnetic lens systems that focus the electron beam. To a certain degree the same optical laws can be applied to condenser lenses and electrons as for the interaction of light with glass lenses. The beam normally travels through more than one condenser lens to achieve a good shape and focus of the beam on the sample surface. Additionally there are apertures between the condenser lenses that remove parts of the beam that are scattered too strongly due to their different energy. The last aperture is the objective lens aperture just above the sample, giving the experimenter the opportunity to change focus and magnification.

Interaction of the Sample with the Electron Beam The images of a SEM originate from different signals that are caused by the interaction of the primary electron beam with the sample. When the primary beam interacts with the sample the electrons lose energy by different scattering and absorption mechanisms. These mechanisms occur in a volume of the sample that has teardrop shape and is called the interaction volume. Depending on the penetration depth and the interaction mechanism different signals can be collected. In Figure 2.9 the interaction volume can be seen showing the different signals and their origin in the interaction volume.

For a standard SEM picture the secondary electrons are detected. As secondary electrons have a small escape depth they allow good topographic information (lateral resolution). Depending on the incident angle of the electron beam on the sample dif-

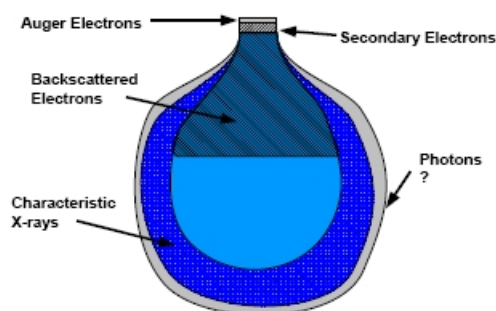


Figure 2.9: The interaction volume of incident electrons. From Waller (2007)

ferent amounts of secondary electrons can escape the sample and reach the detector. This leads to the good topographical resolution that can be achieved through SEM as edges have a different brightness than plains. An effect that limits the imaging of some samples is the accumulation of electrons in the sample if the sample is not grounded. The accumulation causes the image to get brighter until nothing can be observed anymore. One bypass to this problem is by coating the material with a conductive layer (e.g. gold) which leads to good morphologic information but hides certain elemental information.

The detector for the secondary electrons can either be a solid state detector or a scintillator type. Also other signals as X-rays, backscattered electrons or Auger electrons can be found and detected in a SEM, but as they do not contribute to this work they will not be explained any further.

Environmental SEM In standard SEMs all of the inner components where the electron beam passes through must be kept under high vacuum (10^{-9}). This also applies for ESEM except for the sample area.

For ESEM the sample area can be held under various pressures of different gases. However, the beam path through the condenser lenses and the electron source must still be kept under high vacuum. This is achieved through differential pumping with the aid of a small aperture that separates the sample chamber from the beam path. The next difference is that when the primary electron beam travels through the sample chamber it gets attenuated slightly through interaction with the gas molecules. This effect is on the other hand compensated by the fact that secondary electrons from the sample ionise the gas which leads to an amplification of the detected signals. This effect goes hand in hand with another important advantage of ESEM. Whilst for standard SEMs non-conductive materials cannot be observed due to the inevitable electron accumulation on their surface, ESEM allows this due to the imaging gas. The imaging gas has positively charged molecules after the ionization which are attracted by a possible negative charge build-up on the sample surface. The positive charged

electrons tend to neutralize the negative charge making it possible to observe uncoated non-conductive materials. The higher vapour pressure over the sample area also allows one to investigate materials such as ice at temperatures where its vapour pressure would have caused it to evaporate under the pressure conditions of a standard SEM. Comprehensive information on SEM in general can be found in Skoog et al. (2006) and the thesis of Waller (2007) provides further theoretical and practical details of ESEM.

2.5.2 Experimental Setup

The experiments were carried out at the University Service Center for Transmission Electron Microscopy (USTEM) of the Technical University Vienna. The electron microscope used was a Quanta 200 DualBeam-FIB from FEI with ESEM operation mode and built on preparation chamber. The electron source was a tungsten filament.

Sample Preparation For the preparation of the emulsion samples the method of freeze fracturing proved to be a very good way to obtain well observable surfaces in the electron microscope. Therefore, a sample carrier with a hole was filled with the liquid sample over the top, thus producing a drop that looks out of the hole. Then this sample carrier is quench cooled in liquid nitrogen for a minute. Afterwards it is transferred into the cooled preparation chamber of the ESEM. Inside the preparation chamber there is the possibility to manipulate the sample with a cold needle or edge. With the aid of the cold edge the overlapping part of the frozen droplet was broken away revealing a virgin surface with no water ice artefacts from the ambient air.

Measurement Procedure In the measurement chamber the pressure for all emulsions was kept at 0.5 mbar of nitrogen. Starting with a temperature of 170K the sample was then heated slowly and pictures were taken during this process. One of the problems encountered during this step was that the temperature in the sample area increased quickly and not always predictably, so that pictures could not be taken at the exact same temperatures for all samples. The samples were observed until the temperatures got so high that evaporation of the water in the sample was caused, which happened around 230K. One point that needs to be considered is that the electron beam can alter a sample. For the emulsions this effect was observed in one of the first measurements when the beam was focused on one droplet over a time period of 10 minutes with a high magnification. This droplet showed obvious different structures than all the other droplets and evaporated earlier. For the other measurements this effect was tried to be kept at a minimum through short periods of high magnification just while taking the images.

2.6 Inelastic Neutron Scattering

For the investigation of the nitric acid hydrates (N_{Ax}) and their phases the opportunity was granted to perform Inelastic Neutron Scattering (INS) experiments at the Rutherford Appleton Laboratory in Great Britain. INS is a spectroscopic method that is especially sensitive to hydrogen atoms and its bonds making it a great method to apply to hydrates. But before starting an experiment it is necessary to know if the INS spectrum contributes to the understanding of a compound, as the experiment is cost- and resource expensive. An INS spectrum reveals its full information if compared with other vibrational spectra as from Raman and IR-spectroscopy. Additional to XRD measurements these spectra have been recorded previously for the N_{Ax}, making the INS experiments a consequent continuation of the research on these compounds.

2.6.1 Theoretical Background

The neutron is an elemental particle from the atom's core with the approximate mass of a proton but carrying no charge as the proton or the electron does. Neutrons carry a magnetic moment (spin $\frac{1}{2}$) and show wave-particle duality depending on the observed phenomena. Here the effects of the neutrons will be addressed which enables the scientists to generate vibrational spectra with the aid of neutrons. To generate a vibrational spectrum a probe must have a frequency similar to vibrations in the compound to cause resonance. A thermalised neutron has a de Broglie wavelength between 1-5 Å, which is comparable to interatomic and intermolecular distances, and its energy of 30-700 cm⁻¹ is in the range of molecular vibrational energies. These properties make it possible to use neutrons for vibrational spectroscopy. Neutrons are not so easily accessible as X-radiation or electrons. In fact, neutron sources are needed which are large facilities comparable to factories or power plants. Hence the scientist needs to visit such a facility to carry out the necessary experiments.

Neutron Sources Two kinds of neutron sources are existent today. These are nuclear research reactors and spallation sources.

Research reactors were the first invented neutron sources that enabled scientists to use neutrons for different analytical tasks. Even though they have some similarities with nuclear power plants they differ from them by their desired product. Whereas in a nuclear power plant the heat is the desired output, in a research reactor the neutrons are needed and the heat is just an unwanted byproduct. In fact the produced heat is limiting the size and performance of a research reactor as it needs to be guided away safely. In a research reactor thermal neutrons are used to induce fission in a critical mass of Uranium 235 (²³⁵U) which emits high energy neutrons through the fission process.

$${}^1_0n_{thermal} + {}^{235}_{92}U \rightarrow \approx 2.5n_{fast} + \text{fission products} + 180\text{MeV} \quad (2.3)$$

These emitted neutrons are slowed down primarily by the heavy water (D_2O), the water surrounding the core and by different other moderators. Once slowed down they are guided to the experiments through beamlines. Research reactors in Europe are, for example the reactor at the Institute Laue Langevin in Grenoble, France or the research reactor in Munich, Germany both very suitable for carrying out different experiments. One of the problems that comes with research reactors is the need for enriched (${}^{235}U$) which does not occur naturally in high concentration levels. On one hand the production for the (${}^{235}U$) is very cost intensive, and on the other hand it needs high security levels as the (${}^{235}U$) can also be used in nuclear weapons and should stay out of access for abusive elements. A problem that research reactors have in common with nuclear power plants is the final storage for the radioactive waste. This is often discussed, as many of the old final storages proved to be not as final and durable as expected, so there is also the call to keep the radioactive waste to a necessary minimum.

Spallation sources are not as common as research reactors. More than 20 research reactors exist and only 5 spallation sources as yet. The first spallation sources were opened in 1980, years after the first research reactor started up in the 1950s. The mechanism of a spallation source to generate neutrons for analysis is dramatically different from reactor sources. In a spallation source pulses of high energy protons are generated in an accelerator ring and then guided onto a heavy metal target (e.g. tungsten). When a high energy proton hits the target it induces a cascade in the target atoms where elemental particles are set free. Within this process one high energy proton sets free approximately 15 neutrons. The produced heat during this process is much lower than in a fission reactor making it easier to control the temperature. The target is surrounded by a tank of D_2O and water tanks to slow down the fast neutrons. These slowed neutrons are then moderated and are finally guided to the experiments through beamlines. For experiments the major differences to a reactor source are the pulsed neutron beams which have a much higher brilliance than the neutron beam from a reactor. On the other side, the mean neutron flux over time is higher in reactor sources, which is the determining factor for some experiments. The energy amount of the generated neutrons is also quite different; whereas spallation sources generate beams of high energy neutrons, reactor sources produce much more cold and thermal neutrons. This does not mean that one method is better than the other as both have their advantages for certain experimental methods.

For spectroscopic tasks as they were carried out for this work, spallation sources have an advantage because a wider wavenumber region can be covered due to the high energy neutrons generated with a spallation source.



Figure 2.10: The ISIS Rutherford Appleton Laboratory in Great Britain from the air.

Interaction with the Sample Matter If the neutron beam hits the sample it gets deflected for a certain angle that is characteristic for the sample and a certain neutron energy. Neutrons interact with the atom's core in comparison to many other analytical methods which interact with the atom's shell (i.e. the atom's electrons). This is also the reason why materials with many hydrogen atoms show very intense signals in INS. Of all atoms the hydrogen molecule has the best core to shell ratio, resulting in a very good possibility that a neutron gets scattered. This is quite different to many other methods; if we imagine X-rays going through water and being shielded by metals the behaviour of neutrons is contrary. Due to this fact it is no problem to store the samples in aluminium sample carriers as the neutron beam goes nearly straight through the aluminium and gets scattered only by the sample. Coming to the spectroscopic properties of the neutrons it has been mentioned already that all vibrations where hydrogen atoms are involved appear very strong in the spectrum. But also all other signals can be found even though they might appear weak. For neutron spectroscopy no selection rules exist as they do for IR- and Raman spectroscopy. Knowing this, the comparison of INS-Spectra with Raman and IR- spectra is very informative for the scientist working with spectroscopic methods. Standard INS spectra are given in $S(Q,\omega)$ against the wavenumber. The wavenumbers (given in cm^{-1}) can be compared to the wavenumbers in IR and Raman spectroscopy representing the frequency at which atomic bonds vibrate in the molecule. $S(Q,\omega)$ represents the scattering law units given in $(energy)^{-1} S(Q,\omega)$

Further information on theory and applications of INS can be looked up in Mitchell et al. (2005)

2.6.2 Experimental Setup

The measurements for this work have been carried out at the TOSCA experiment at ISIS Rutherford Appleton Laboratory in Didcot, Great Britain. Dr.S.F.Parker was the supervising scientist of this experiment. The aim was to gain spectra of the different phases of the NAX species. For this task different concentrations of nitric acid were prepared in an amorphous state. If it proved to be amorphous an annealing procedure was started in order to crystallize the sample and spectra were taken again. The TOSCA setup is equipped with a forward- and a backscattering analyser. It is also equipped with a cryostat that cools the sample area indirectly over the surrounding gas. This makes it possible to make exact annealing programs to observe phase changes in compounds. To obtain good spectra it is beneficial to measure for at least 6 hours, even though certain parameters as the amorphicity may be determined earlier in spectra with lower resolution.

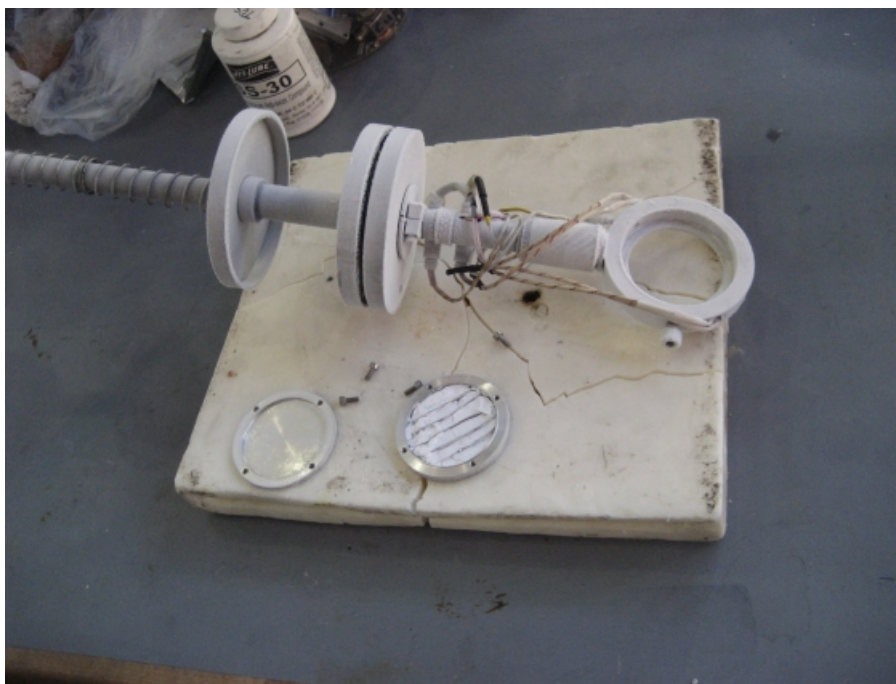


Figure 2.11: The INS sample holder rod

2.6.3 Experimental Procedure

For the measurements of the nitric acid monohydrate (NAM), solutions of 50 mol% nitric acid were prepared and controlled by titration. These solutions were then quenched in liquid nitrogen as explained in Section 2.2.2. The sample was brought into the aluminium sample carrier under liquid nitrogen and closed under liquid nitrogen as well. The sample carrier was mounted on the end of a long rod that was then

plunged into the cryostat of the TOSCA experiment. All these steps had to be carried out with the caution not to conduct heat to the sample. Necessary steps were the precooling of screwdrivers and tweezers before manipulating on the sample carrier or the sample. Also the time when the sample rod was taken out of the liquid nitrogen bath and transferred into the cryostat was kept at a minimum. The temperature in the cryostat was at 20K, ensuring that the sample does not react or crystallize. When the rod was fixed the measurement of a spectrum was started to see if the sample was amorphous. It took about 20 minutes to make the decision if amorphous sample was present. After initial problems to produce amorphous sample matter for the first experiments, the spray-quench method proved to function every time without fail, making this task much easier. If amorphous sample was present the spectrum was measured for a longer time (e.g. 4 hours); if not, the sample was discarded. When a good spectrum of the amorphous phase was gained the annealing procedure was started with heating up to 220K in the case of NAM, and a 2 step annealing in the case of NAT to 160 and 220K. After reaching a temperature where phase change was expected the sample was cooled down again and a spectrum was taken for about 6 hours. For the NAT an additional modification of the sample carrier needed to be done to gain access to the metastable α -phase. A crude grid made of aluminium foil was placed into the sample carrier as it is seen in Figure 2.11. This prevented the amorphous sample from aggregating too much when placed vertically into the cryostat. Without this grid only the β -phase spectrum could be observed after annealing. One explanation for this might be that the change from the amorphous material to the crystalline hydrate went hand in hand with an observed increase of the sample volume. When aggregated the sample possibly experienced regional pressure increases which led to a preference of the β -phase. Even though this explanation is only an idea it is a fact that the process works with the grid.

Chapter 3

Results

3.1 X-Ray Diffraction

3.1.1 Diffractograms

The measurements of the citric acid emulsions have been carried out at a stable temperature of 190 Kelvin. The temperature was stable within a range of $\pm 1^\circ$. In Figure 3.1 all diffractograms have been plotted into one graph. This helps to visualize the change of the patterns (i.e. the phase composition) as well as the shape of the reflexes (i.e. the texture and the geometry of the crystallites). Obviously for pure water ice, sharp reflexes with nearly no background occur. With increasing citric acid concentration the reflexes are getting broader and the background signal grows up which is related to amorphous material remaining.

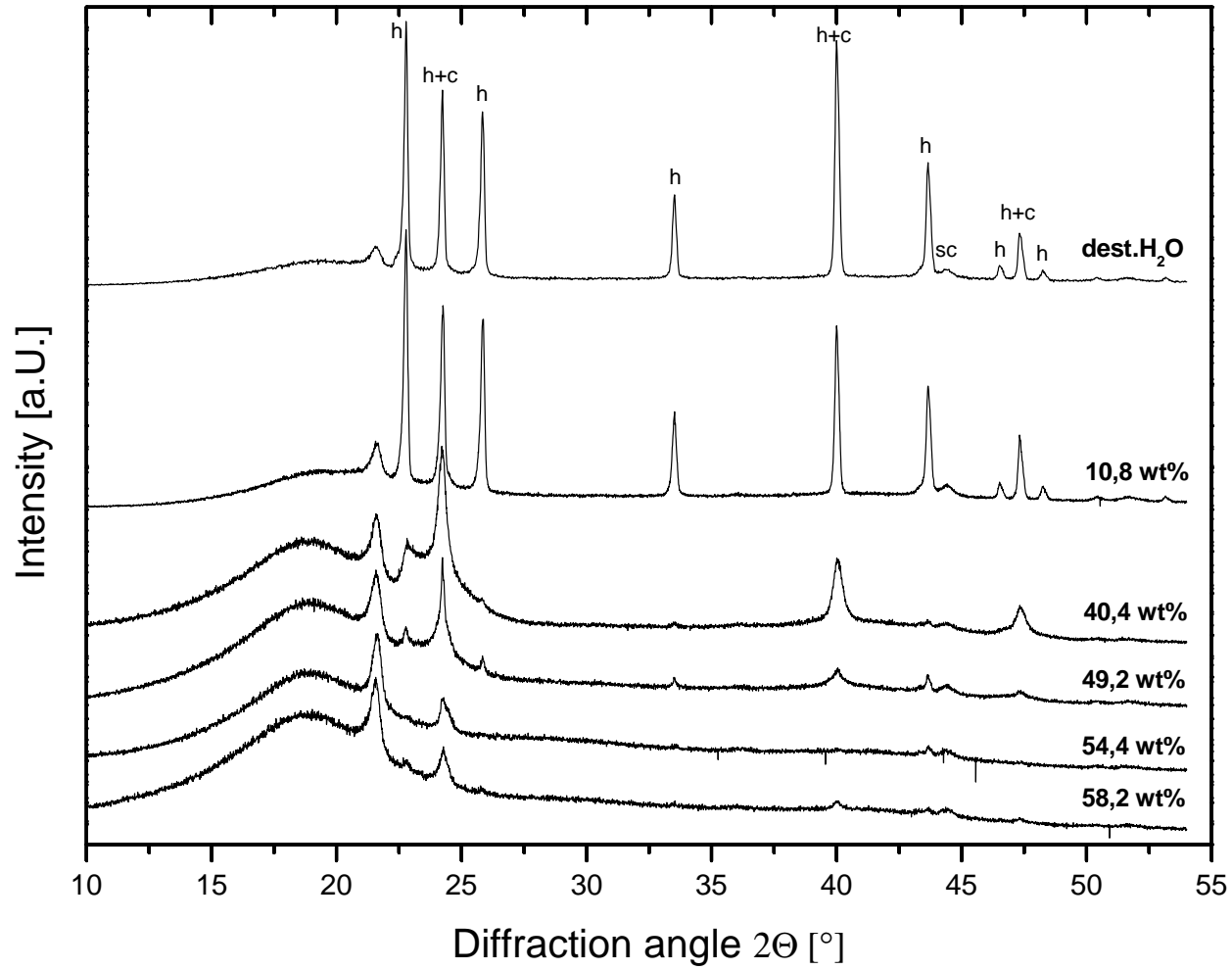


Figure 3.1: XRD results for the emulsions at 190K

Starting with the uppermost diffractogram which shows pure water in the emulsion, the citric acid concentration is increasing downwards. The prominent peak reflexes for ice have been named with "h" for reflexes of the pure hexagonal crystal structure (I_h) and "h+c" for those reflexes that are connected to the hexagonal and the cubic modification (I_c) of water ice. The reflex of the sample carrier is named with "sc". When comparing the reflexes the intensity and sharpness of the hexagonal modification reflexes is decreasing with the increasing citric acid concentration. In contrast, the reflexes that can be assigned to the mixed phase (I_h and I_c) stay strong. This is an indication for the presence of more cubic ice crystals and a higher grade of disorder in the structure.

3.1.2 Rietveld Analysis

For the phase determination of the sample Rietveld analysis was carried out with the data of the diffractograms presented in Section 3.1.1. The exact output documents can be found in the Appendix, as they do not contribute very much to readability here. As a useful byproduct the Rietveld analysis also calculates the crystallite sizes in the different phases.

The results for the crystallite sizes are summed up in a figure showing the crystallite size plotted against the citric acid concentration. The error bars were generated from the highest error that showed up in different calculations to reduce misleading guesses about the accuracy of the crystallite size. By having an eye on the error bars it can be said that information on the absolute crystallite size is poor.

For the comparison of the crystallite sizes in different samples the results are still expedient and a trend to smaller crystallites with higher citric acid concentration can be observed.

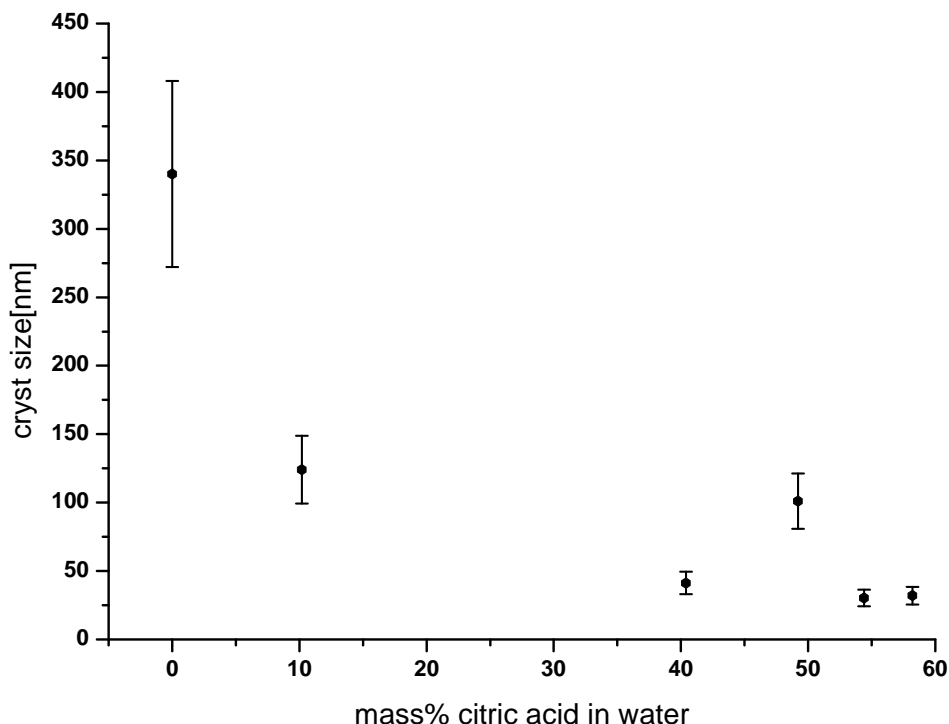


Figure 3.2: Calculated crystallite sizes for Ice I_h

3.2 Raman Spectroscopy

For the Raman spectroscopic measurements the setup and procedure is explained in Section 2.4.2. The measurements themselves proved to be more difficult than it was initially thought. Due to this some encountered problems have to be named and also the limits of the method and setup need to be discussed.

3.2.1 Difficulties and Limits

The problems with measuring droplets in an emulsion have been mentioned briefly in Section 2.4.2, but will be explained here further to make clear what information can be extracted from the spectra.

The Raman spectrometer is equipped with a confocal microscope that focuses the laser beam in the desired plane of the sample. For solid crystalline samples this is mostly an easy task to perform if the focus is laid onto the surface. For liquids it is already a bit more sophisticated, but still possible if the liquid sample is thick enough and distinguishable from its sample carrier. The focus should therefore lie within the

liquid sample. To take spectra of droplets in emulsions the difficulties increase even more. To get a good spectrum of a droplet the focus of the laser should obviously lie within the droplet.

If the emulsion is now still liquid (i.e. at room temperature) one of the encountered problems was that the droplets were moving due to a spreading of the emulsion between the glass covers where it was kept in. The movement slowed down after a short time but never came to a full stop. This fact was limiting the measurement time and through this the quality of the room temperature spectra. If the droplet is captured nearly steady another problem arises. To set the focus in the sample a light microscope is used to find the right spot and plane. Sadly, the contrast between the droplets and the oil matrix of the emulsions is only poor, as can be seen on the picture in Figure 3.3 which was taken with the best achievable contrast for this sample.



Figure 3.3: The emulsion with 49,2 wt% citric acid under the light microscope of the Raman spectrometer

If the difficulties with the contrast are taken into account it is clear that problems as they are explained in Figure 3.4 may arise. But even if the focus lies correctly, the spectrum is still influenced by the surrounding of the droplet even if this is kept at a minimum. So in reality the spectrum itself contains vibrational information not only of the droplet but also of the oil and even the bottom beneath. In the case of this measurement series the spectrum of the ceramic surface from the Peltier cooling stage always interferes with the desired spectrum of the droplet.

When working with spectroscopic data one common solution to get rid of such undesired information is the recording of a background spectrum. This can then be subtracted from the sample spectrum to gain a spectrum with only the desired information left. For these measurements it would be a background spectrum of the oil matrix and the ceramic surface. The problem that arises is that this method works only under the condition of a stable background intensity. For the sample material that was used here the intensity is always changing, depending on the size and proximity of the droplet, the transparency of the sample (which changes with temperature) and the exact thickness of the sample. Unfortunately these factors are beyond reproducibility with this setup.

Before these difficulties became clear there was the attempt to make a spectroscopic

mapping of the droplet. This could have revealed differences within the droplet after the freezing process. Especially the effect of "brine concentration" was hoped to be observed. This was not possible due to the explained limits of the method and the setup. Still, some useful information about the freezing differences between the emulsions can be extracted and will be presented here.

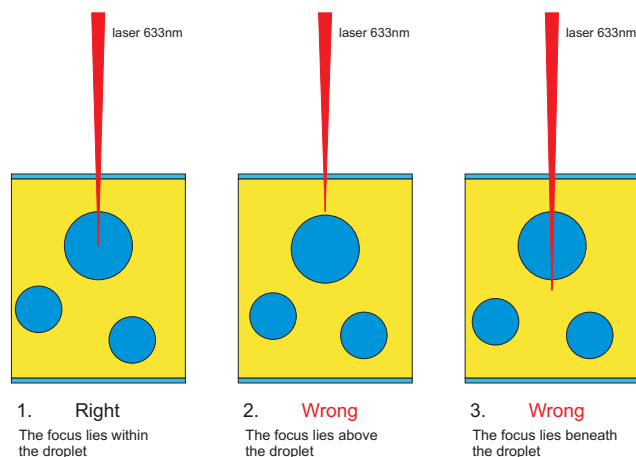


Figure 3.4: Different error sources: Case 1. shows where the focus of the laser should lie to receive the desired spectrum. The problem with focusing the droplet correctly may lead to the Cases 2. and 3., which would lead to an unwanted spectrum.

3.2.2 Raman spectra

Before the Raman spectra of the emulsions are discussed a spectrum of water and ice is presented where the important differences of the liquid and the Ice I_h phase are pointed out.

The spectrum in Figure 3.5 has two points of interest concerning the Ice I_h . These are the bands situated at $\approx 225\text{cm}^{-1}$ in the translational vibrations region and at $\approx 3150\text{cm}^{-1}$ in the region of the -OH stretching modes. The other strong bands around 1500cm^{-1} are from the sample carrier and they lose intensity, as the ice phase has a lower transparency than the liquid water phase. These two interesting bands can now be observed and analysed in the different emulsions as they act as a good sign for the existence of Ice I_h .

The spectra in Figure 3.6 are in good accordance with the behaviour that is expected when knowing the X-ray diffractograms. The band at $\approx 3150\text{cm}^{-1}$ is losing intensity with an increasing content of citric acid in the aqueous phase. In fact it is nearly gone at the spectrum with 40,4 wt% even if a broader but weaker band can still be seen in its place. The broadening of the band in combination with a decrease of the intensity is a sign for an increasing grade of disorder in the ice structure. Unfortunately the uppermost spectrum in Figure 3.6 had a change in intensity during the

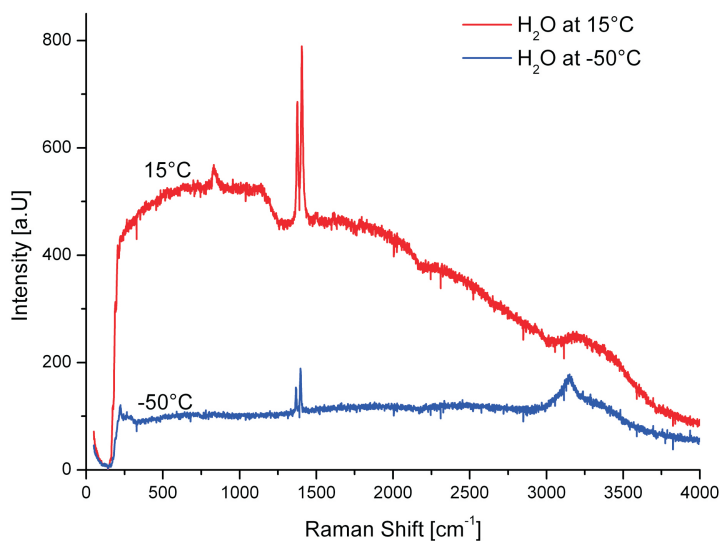


Figure 3.5: The Raman spectrum of water and of Ice I_h

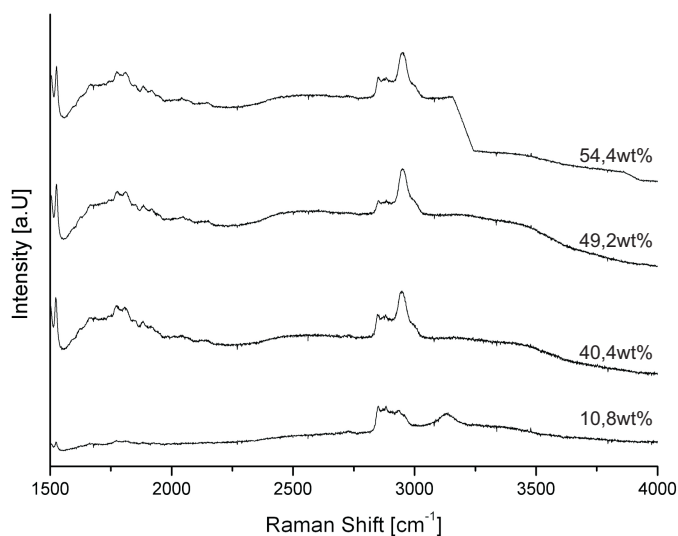


Figure 3.6: The Raman spectrum of the samples in the higher frequency region. The wt% give the amount of citric acid in the aqueous phase

measurement. This produced a disturbing step in the spectrum but fortunately the $\approx 3150\text{cm}^{-1}$ band lies just before the step so that the amount of information needed here is not affected.

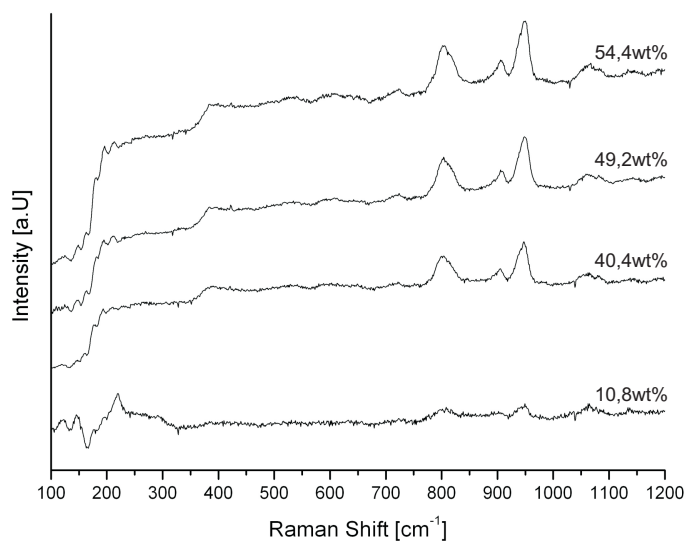


Figure 3.7: The Raman spectrum of the samples in the lower frequency region. The wt% give the amount of citric acid in the aqueous phase.

Also the low frequency region spectra in Figure 3.7, with the characteristic ice band at $\approx 225\text{cm}^{-1}$, follow the trend that is observed in Figure 3.6. In the emulsion with 10,8 wt% citric acid the band is clearly seen, and in the following spectra with higher concentrations of citric acid the band broadens and then disappears. These results support the idea that the citric acid is an agent that is highly capable of disturbing the structure of water ice.

3.3 ESEM

The samples of citric acid emulsions were observed with the electron microscope according to the setup and preparation method explained in Section 2.5.2. The contrast and quality of the ESEM pictures are unevenly higher than those made with the light microscope of the Raman spectrometer, making it possible to distinguish between different domains in the droplet. Interesting different morphologies were found in the different samples that could be correlated with the different concentrations of citric acid in the water phase.

Besides this scientific information the electron microscopy revealed beautiful miniature landscapes and patterns that do not lack aesthetic qualities.

3.3.1 10,8 wt% Citric Acid in Water

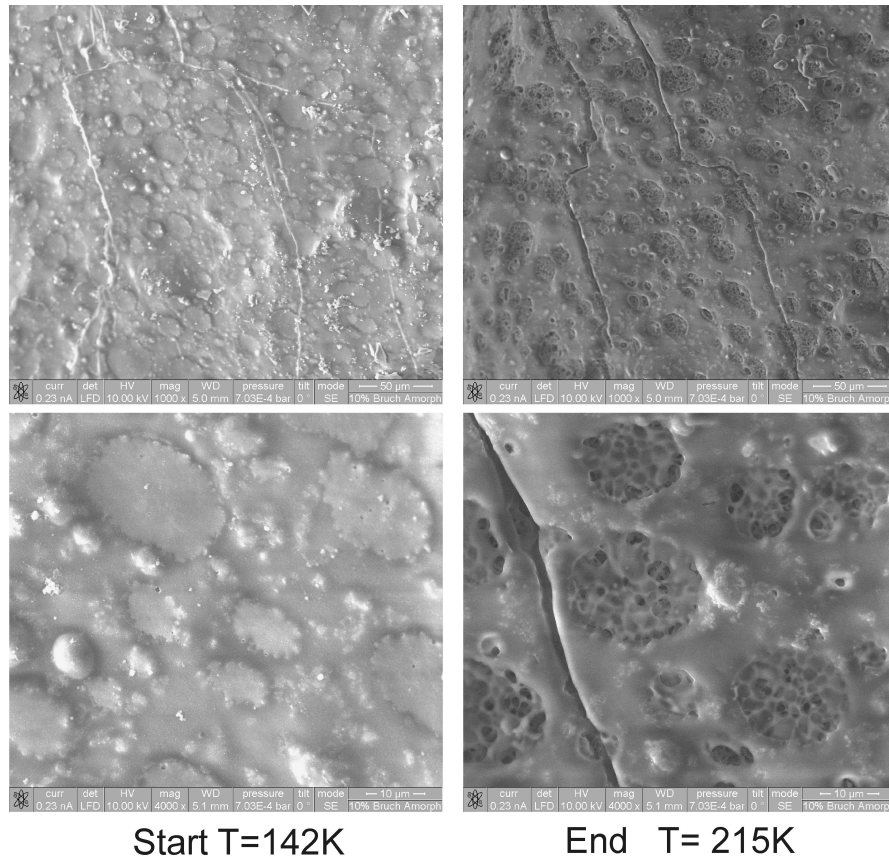


Figure 3.8: Emulsion with 10,8 wt% citric acid before and after evaporation of the water in the sample leaving a structure of probably citric acid that does not evaporate

This sample needed to be prepared three times, as one time the cutting of the sample in the preparation chamber failed and the other times the temperature rose

too high (over 180K) before a plain spot for observation could be found on the sample surface. After these first obstacles the sample could be observed without further problems. The droplets could be distinguished easily from the oil matrix and were in the expected size between 10-20 μm . From the information of the XRD measurements it was expected that the droplets would be crystalline. This could hardly be decided from the first look at the sample which was at approximately 130-140K. Two pictures from this stage are shown in the first part of Figure 3.8. After warming up a little to 160K, structures became visible within the droplets that gave evidence of crystalline structures. A picture at 180K is shown in Figure 3.9 where a netlike crystalline structure is present.

As the sample was prepared by dipping into liquid nitrogen and then transferring it into the electron microscope it is expected that the droplets in the sample are amorphous and crystallize during the annealing process in the chamber.

Another explanation why the structures are not visible instantly is that a thin film of water that comes from the sample is recondensing on the sample surface as a stable vapor pressure over the sample is reached. Through an increase of the temperature this film evaporates again and perhaps even a little of the ice below, allowing a clear view and good contrast in the sample. When the temperature increases further above 210K the water in the sample evaporates, leaving behind a weblike structure of what is probably citric acid (monohydrate).

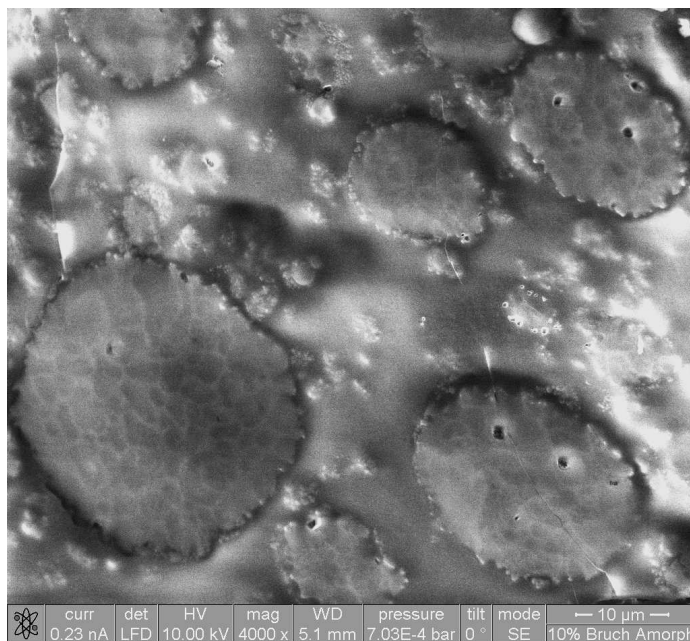


Figure 3.9: The emulsion with 10,8 wt% citric acid shows crystalline like patterns within the droplets at 170K

3.3.2 40,4 wt% Citric Acid in Water

The 40,4 wt% was expected to be crystalline, as the diffractogram shows crystalline phases, even though to a smaller amount than for the 10,8 wt% emulsion. In the ESEM the sample behaved much like the 10,8 wt% emulsion, revealing crystalline patterns during the annealing process. The crystals appear to be larger than in the previous emulsion, which might lead the observer to the conclusion that in 40,4 wt% emulsions the crystallites are larger. Even though one might be tempted to make this conclusion from looking at the picture, it has to be kept in mind that ESEM is not a method that gives exact information on crystallographic parameters, but morphological information. As the XRD gave evidence that the crystallite size is decreasing with increasing acid concentration, the conclusion arose that many small crystallites contribute to the structure that is observed in the ESEM picture seen in Figure 3.10 .

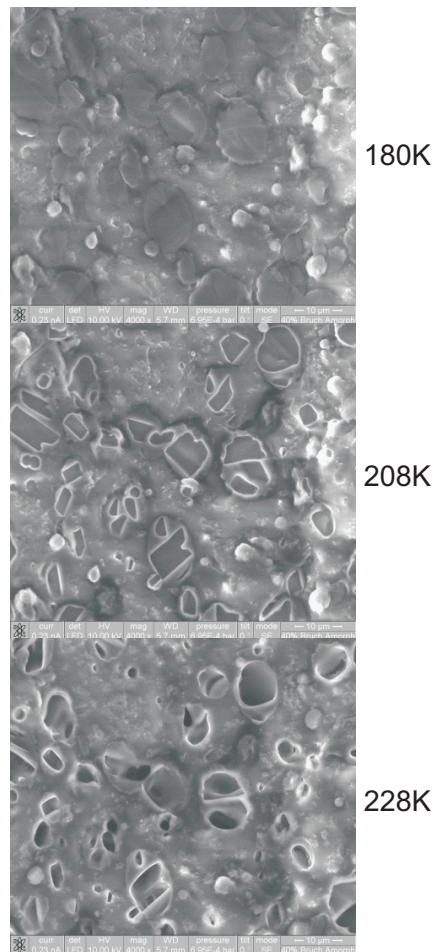


Figure 3.10: The same spot in the 40,4 wt% is observed at increasing temperature. After 5 minutes at 228K the water in the emulsion seemed fully gone leaving behind a cavelike structure.

3.3.3 49,2wt % Citric Acid in Water

The 49,2 wt% CA sample behaved a little differently than the previous emulsions, as no obvious structures could be observed within the droplets that would give evidence of crystalline phases. Also, no structures could be seen at 228K where the water of the droplets should be evaporated, leaving behind the citric acid. Instead of the net- or cavelike structures that were observed in the samples with lower CA concentration, it seems that in this sample just a more or less thick film of citric acid (monohydrate) is left after the water has evaporated.

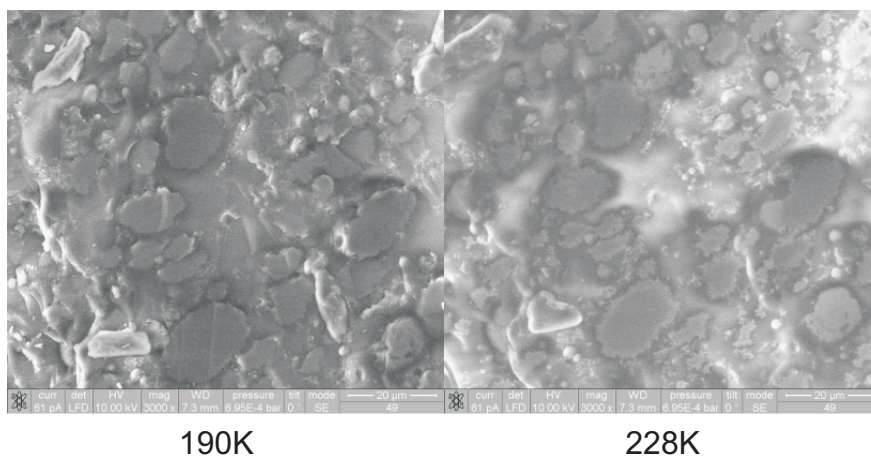


Figure 3.11: A spot in the sample with 49,2 wt% citric acid is observed. No obvious structures seem present that would give a clue of crystalline phases.

3.3.4 54,4 wt% Citric Acid in Water

During the warm up process a film of water ice was present on the sample which seemed to result from recondensation of water from the sample material. This film lasted for a temperature period of approximately 30K between 170K and 200K. The evaporation of this water film and a change of the droplet's appearance through evaporating water could be observed. The emulsion with 54,4 %wt citric acid showed no special leftover structures after the water in the sample was gone. The citric acid appears as a leftover film in the droplet. This compares well with the XRD results as only traces of the crystalline phase should be present at this concentration.

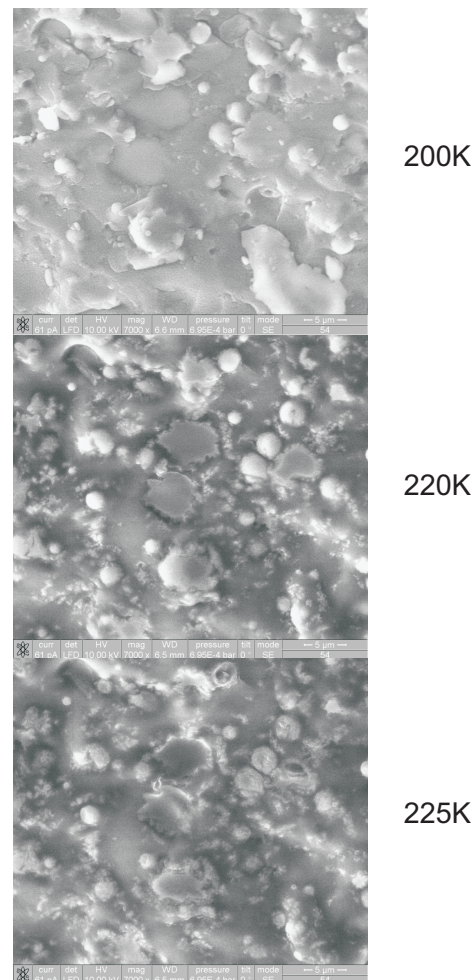


Figure 3.12: During the annealing of the emulsion with 54,4 wt% CA evaporation of the water could be observed. Characteristic structures did not evolve.

3.3.5 59,2 wt% Citric Acid in Water

The emulsion with 59,2 wt% citric acid behaved very similarly to the one with 54,4 wt% citric acid. No crystallization event could be observed and a thin film was left after the water evaporated. The sample itself drifted during the observation. So pictures were not taken at the same spot. Anyway, as the behaviour of the droplets is the same all over the sample the information content is not decreased through the drift.

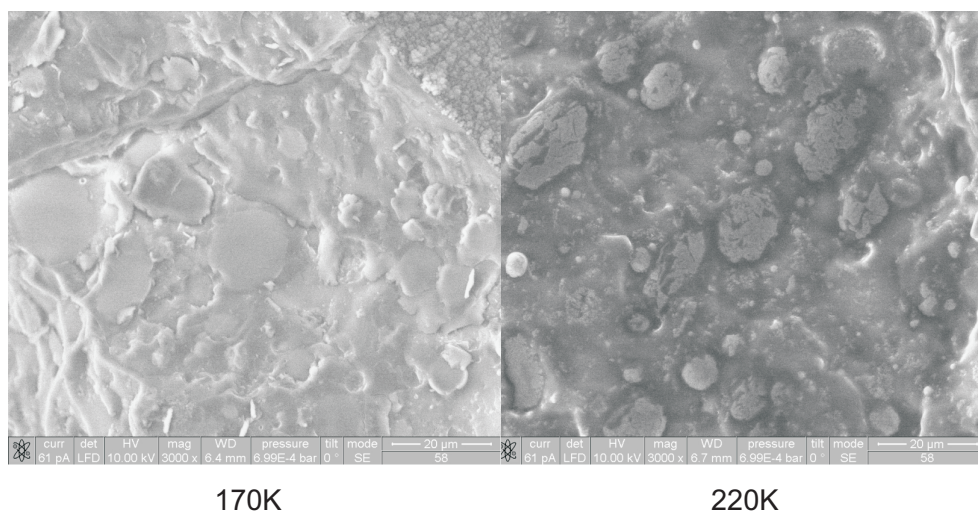


Figure 3.13: Sample with 59,2 wt% citric acid in water. The first picture at 160K is covered by an ice film. On the second picture the water from the droplets is evaporated already and a film of citric acid is left behind.

3.4 Inelastic Neutron Scattering

Two different concentrations of nitric acid solutions have been analysed which refer to the compositions of nitric acid monohydrate (NAM), and nitric acid trihydrate (NAT). The preparation of all samples and the measurement procedure followed the steps explained in Section 2.6.2 and 2.6.3

3.4.1 NAM

The collected data for the NAM is summed up in Figure 3.14 where the important spectra are connected in one diagram making it easier to observe the phase change.

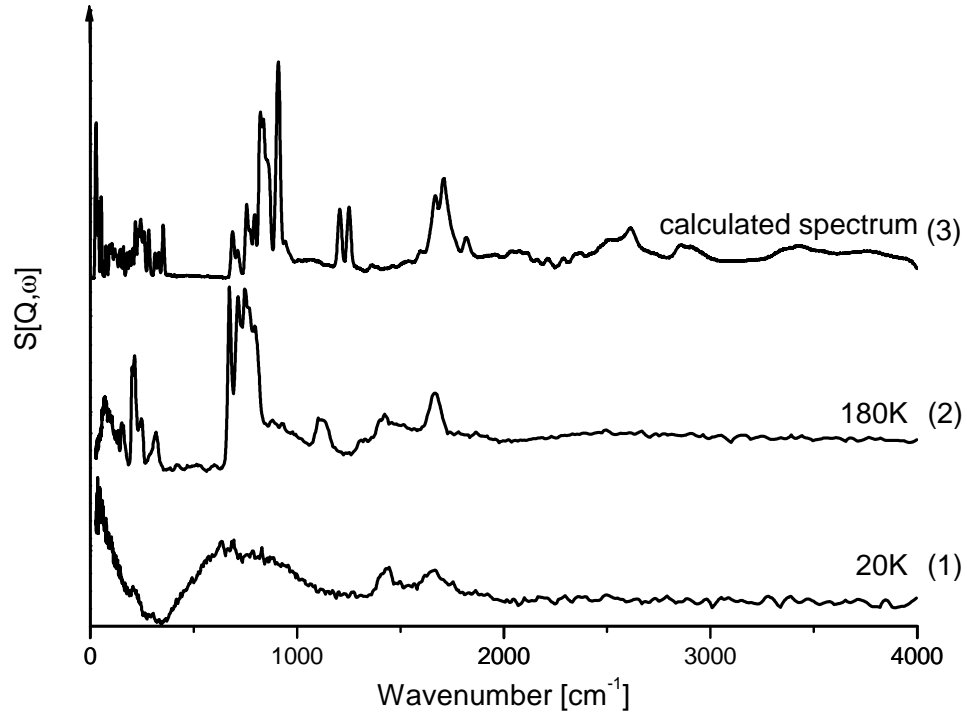


Figure 3.14: NAM evolving from an amorphous phase of 50 mol% nitric acid through annealing.

According to the measurement procedure explained in Section 2.6.3 the spectrum labeled with 20K is the first spectrum that was taken of the sample just after it was brought into the cryostat. At this stage the sample is present in an amorphous state and has not experienced annealing. The spectrum obviously shows no strong single bands, but a wide background structure which is a sign for a non-existent long range order, i.e. amorphicity.

In the phase diagram the NAM shows only one phase and XRD measurements revealed that it is fully descended into this phase after annealing to 180K. The spectrum labeled with 180K is also taken at 20K, but after annealing for 30 minutes at 180K and fast cooling back to 20K for the recording of the spectrum. In this spectrum a structure with many strong single bands can be seen and the difference to the spectrum of the amorphous phase is striking.

The uppermost spectrum is a calculated spectrum generated from a previously re-

ported DFT calculation by the program ACLIMAX at the Rutherford Appleton Laboratory. It is common to many theoretical calculations that they are either blue- or redshifted, which seems to apply for this spectrum which is a little blueshifted. However, the theoretical spectrum was generated to have an orientation of how the INS spectrum of NAM may look and serves well for this task. If the look is directed onto a certain region with more accuracy, the calculated spectrum does not apply too well any more. The poor agreement between the observed and calculated INS spectra arises from the use of an inadequate model. Unfortunately such better model calculations were beyond the resources of this work.

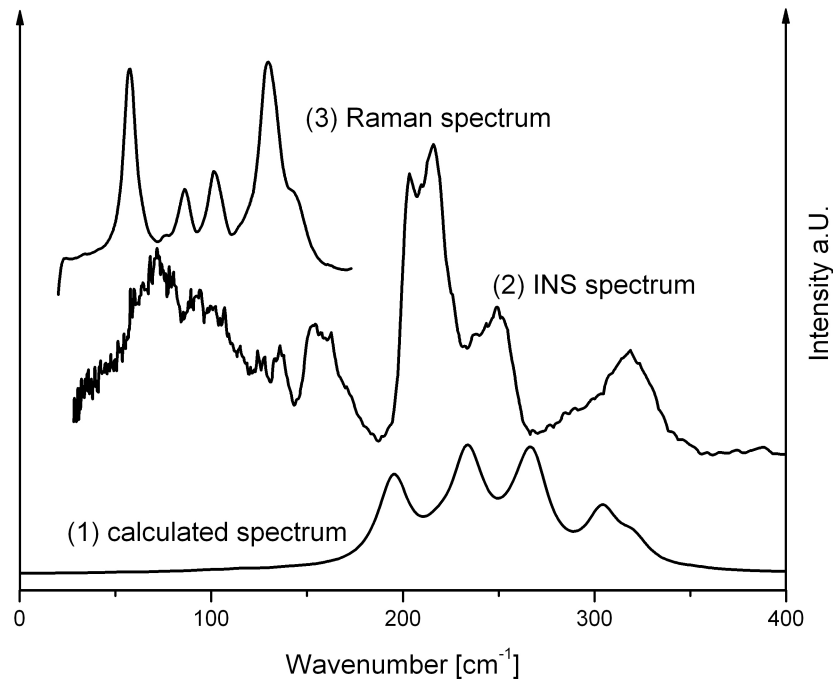


Figure 3.15: A comparison of the low frequency range of NAM in a Raman, INS and calculated vibrational spectrum.

For Figure 3.15 the low frequency region of the INS Spectrum of NAM was compared with another ab initio calculation and a Raman spectrum that was taken by Grothe et al. (2006a) to investigate the low frequency region.

All three spectra seem different at first glance, as corresponding to the diverse techniques used in each case. All vibrations where hydrogen is involved produce a strong signal in the INS spectrum, whereas in the Raman spectrum all vibrations which involve the movement of an oxygen atom are more intense due to the favoured change in polarizability, which is related to the higher electron density of oxygen than of hydrogen. Nonetheless, the band distribution shows some similarities between Raman

and INS in the lower part of these spectra, and also between INS and IR in the higher frequency region. Analysis of the calculated IR spectrum indicates that most of these vibrations can be described as in-phase and out-of-phase twisting of the NO_3^- group and flattening of the H_3O^+ part. This information can help with further band assignment in the future.

For the region up to 2000 cm^{-1} some bands have already been assigned in previous publications which will be compared with these results. Especially IR measurements were carried out which have served as reference spectra for many years. They can be used to compare with the INS spectra as the appearing bands must be present in the INS spectra even though with different intensities. INS measurements have been carried out as well, Janik et al. (1968).

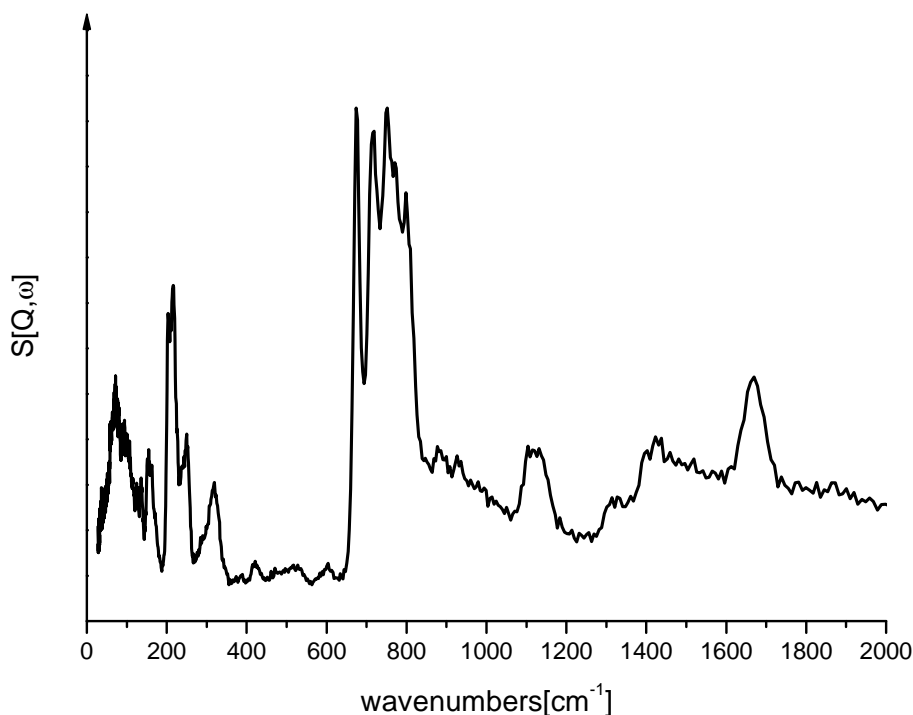


Figure 3.16: Spectrum of NAM taken at 20K after annealing to 180K.

In Tables 3.1 and 3.2 the data of previous papers is listed and compared with the INS data from this work. The data is derived from the spectrum shown in Figure 3.16.

The INS spectrum compares well with previous INS spectra by Janik et al. (1968). In addition to the bands that have been mentioned in Janik et al. (1968), other bands were found in this work as a result of the higher resolution of this spectrum, which enables one to distinguish better between bands which are close to each other. At

INS ^a	Raman ^b	INS ^c	Assignment ^c
59	58		
70	75		
90	86		
	101		
124	118	112	opt.trans vibration of H ₃ O ⁺
135	129		
154	143		
162		164	
203		206	T _x
216			
238			
249		246	T _y
300			
318		321	T _x +T _z
387			
421			

Table 3.1: ^a INS data from this work, ^b Raman data from Grothe et al. (2006a), ^c INS data by Janik et al. (1968), ^d assignments by Janik et al. (1968).

758cm⁻¹, for example, Janik et al. (1968) found one broad band, whereas about 6 different bands can be distinguished in this new spectrum. The bands from the IR reference data can also be found, and especially the H₃O⁺ bands are observed with strong intensities in the INS spectrum as in the band at 673cm⁻¹. The band assignment has been done for some of the bands in the IR and INS spectra already and can be looked up in Table 3.2. The assignment is helpful but still far from being complete. The gained INS spectra may contribute to further band assignments in the future.

INS RAL ^a	IR ^b	IR ^c	IR ^d	IR ^e	Raman ^f	INS ^g	Assignment ^h
603							
673		675	670	680			H ₃ O ⁺ torsional vib.
	702	700		702			H ₃ O ⁺ librational ν_1
718	721	723	723	722			NO ₃ ⁻ asymmetric bend ν_4
	735	737	738	735			NO ₃ ⁻ asymmetric bend ν_4
750						758	R _x +R _y vibration of H ₃ O ⁺
770	780			775			
798	814	815	816	813			NO ₃ ⁻ symmetric bend ν_2
877							
926							
969							calc.NO ₃ ⁻ symmetric stretch ν_1
					1044		
					1055		
1103	1102						
1114				1115			H ₃ O ⁺ symmetric bend ν_2
1131	1135	1135	1134				
	1279			1260			NO ₃ ⁻ asymmetric bend ν_4
1314				1316			NO ₃ ⁻ asymmetric bend ν_4
1327							
1402		1386	1361				
1423							
1437							
1459							
1669	1674	1680	1670	1671			H ₃ O ⁺ asymmetric bend ν_4

Table 3.2: ^a is the INS data from this work, ^b IR data by Ritzhaupt and Devlin (1991), ^c IR data by Savoie and Giguere (1964), ^d IR data by Bethell and Sheppard (1953), ^e IR data by Smith et al. (1991), ^f Raman data by Grothe et al. (2006a), ^g assignments are summarised from all sources mentioned here.

3.4.2 NAT

. According to previous XRD and FTIR measurements the NAT shows two different phases: the α -NAT and β -NAT phase. The Alpha phase is a metastable phase and can only be observed below 200K. If heated further the α -NAT phase irreversibly descends into the β -NAT phase. This phase change could be observed very well with INS spectroscopy. The spectra of the three phases (amorphous nitric acid, α -NAT and β -NAT) are shown in a diagram in Figure 3.17

An assignment of the bands as shown for the NAM was not done for the NAT in this work. The different NAT spectra are rather used as fingerprints to distinguish between the phases with the aid of vibrational spectroscopy.

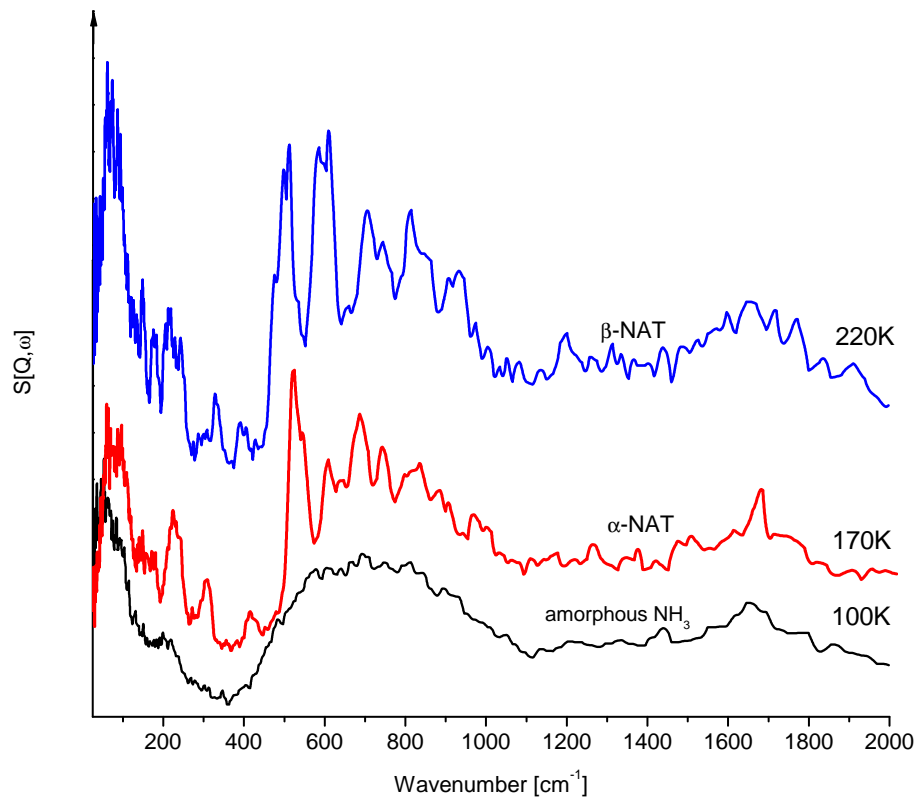


Figure 3.17: INS spectrum of α -NAT and β -NAT evolving from an amorphous phase due to annealing.

Chapter 4

Discussion

4.1 Cirrus Cloud Models

The use of an emulsion as the model system worked well for most of the desired tasks. The setup of the experiments was aimed to partly simulate upper tropospheric conditions by using similar cooling rates and temperatures, which was mainly achieved as well.

By recalling the questions that were asked in Section 1.5 it can be discussed as to which answers could be found and which questions do need further research.

4.1.1 Does Citric Acid Suppress the Nucleation of Ice?

The previous works of Murray (2008a) already mentioned that citric acid is able to cause water ice to stay amorphous at tropospheric conditions. This is clearly confirmed by the experiments that were carried out here. Primarily the XRD measurements showed the same results, just to be underlined by the Raman spectrograms. The effects could be observed step by step in the diffractograms in Figure 3.1 where the bands broaden with the increasing concentration of CA until the concentration of 58,2 wt%, where the reflexes for Ice I_h have nearly disappeared. Instead of sharp reflexes one broad reflex is left, which is a sign for a highly disordered structure which equals amorphicity.

Also the spectroscopic investigations with the Raman spectrometer showed a loss of signs for Ice I_h with the increasing CA concentration.

Overall it can be said that the grade of disorder in the water ice increases with increasing citric acid concentration until nearly no crystalline phase is left and amorphicity is present. As one nucleation event itself is hardly recognised, it may be that some nuclei have come together, but in practice the citric acid does effectively suppress crystallization in water ice.

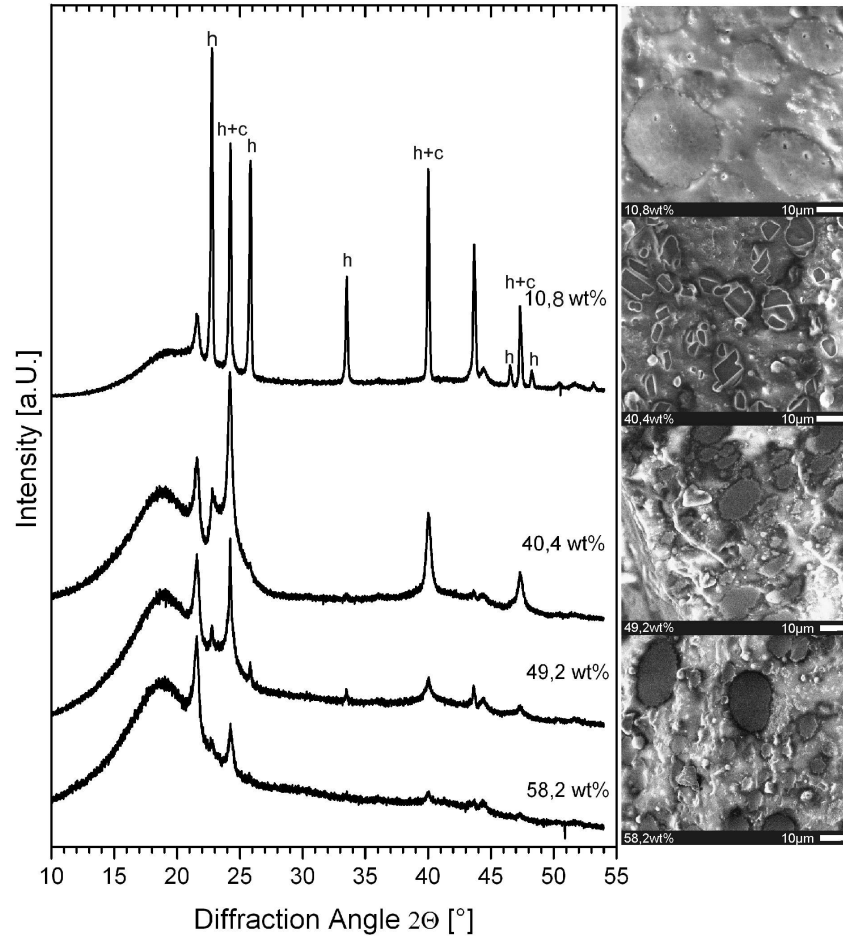


Figure 4.1: XRD and ESEM data of selected samples

4.1.2 How does Citric Acid Influence the Phase Composition in General?

In the XRD we can see that in the sample with pure water the reflexes of the Ice I_h pattern are present sharp and strong. This changes with the increasing CA concentration where the I_h reflexes lose intensity and a broad background signal increases at their expense. Also certain reflexes, which are part of the I_h pattern, remain strong. These reflexes are combined reflexes of Ice I_h and Ice I_c (i.e. the hexagonal and the cubic modification of ice). Since the intensities of XRD patterns are connected with each other, the fact that these reflexes stay strong must root in the contribution of the cubic ice modification. These reflexes are still strong at 49,2 wt%CA and lose their intensity only at very high CA concentrations. The general pattern that can be

retrieved from these observations is that with increasing CA concentrations the Ice I_c modification is preferred over I_h and the amorphous phase is preferred over I_c at very high CA concentrations.

4.1.3 If Nucleation Occurs How Does Citric Acid Affect the Crystal Growth?

Especially in the samples with lower CA concentrations, signs for the crystalline phase of Ice I_h are still present. Thus nucleation must have occurred in a sufficient amount. If the calculations of the Rietveld refinement in Section 3.1.2 are interpreted, they reveal a trend to smaller Ice I_h crystallites with increasing CA concentration. As already mentioned, the amorphicity of the sample increases with higher CA concentrations. This brings up the assumption that the development of smaller crystallites and thus a higher grade of disorder is preferred with higher CA concentrations. Further propagation of the crystal structure to larger crystallites seems hindered, with an efficiency that is directly proportional to the CA concentration. With hindered crystal growth the space between the crystallites is left in an amorphous state.

4.1.4 Is the Morphology of the Sample Influenced by Citric Acid?

The use of the Environmental SEM in combination with the preparation method made it possible to observe the inside of the droplets in the emulsion with an as yet unexperienced contrast and brilliance. The different morphologies of the samples could be clearly pointed out, as is seen in Section 3.3. The ESEM pictures can also be interpreted as some kind of a mapping of the sample, even if it is not by spectroscopic means. The different regions of brightness (which are connected to the amount of electrons escaping from the spot) make it possible to draw conclusions about the distribution of the CA in the frozen samples. Those samples that did still crystallize sufficiently (which are those under 49,2 wt% CA concentration) showed beautiful structures and spots where the CA seemed to concentrate during the freezing process. This effect of brine concentration is known of salts as well, which are concentrating in a freezing solution at the front of a propagating crystal structure.

At the higher CA concentrations no more structures could be observed, but a rather homogeneous droplet. This could be rooted in the fact that the remaining crystallites might be very small and distributed randomly in the droplet, whereas most of the droplet is amorphous water.

It can be concluded that the amount of citric acid strongly affects the morphology of the samples, but a trend to certain patterns could not be pointed out other than by dividing the samples into mostly amorphous and mostly crystalline ones. Within one sample all droplets showed the same structures, but it can't be excluded that in another sample with the same CA concentration, slightly different structures may oc-

cur when different cooling rates or temperatures are applied. In Figure 4.1 XRD data is connected with the ESEM pictures for a better visualization of the diffractograms and their associated ESEM pictures.

4.1.5 What Helpful Spectroscopic Information Can Be Extracted for a Better Understanding on the Molecular Level?

The Raman spectroscopy brought some fine results, but not the full potential of the spectroscopic information could be tapped due to the difficulties explained in Section 3.2.1. The samples could be distinguished well from each other and also the trend to a higher disorder with increasing CA concentration could be found. Unfortunately many parts of the spectra were interfered by the background spectrum signal of the ceramic Peltier surface and the oil matrix that surrounded the droplets. The characteristic Ice I_h signals could still be found and their decrease acts as a clear sign for the loss of the hexagonal structure. A spectroscopic mapping of the sample failed due to the too low lateral resolution of the laser. Also more information on the spectroscopic differences between I_h and I_c were hoped to be gained but remained hidden. This may be solved in the future with a different model system as emulsions do not seem to be the most adequate model for Raman spectroscopy.

4.1.6 Conclusions

In brief the following conclusions can be drawn from the experiments.

- Citric acid interferes with the ice nucleation process.
- Citric acid seems to promote cubic ice nucleation in comparison to hexagonal ice.
- Crystal growth of ice is suppressed by citric acid.
- At high citric acid concentrations ice nucleation seems suppressed.

4.2 INS on Nitric Acid Hydrates

The inelastic neutron scattering experiments on the nitric acid hydrates provided mostly new and good spectra that have not been recorded before. The amount of information gained here will serve as a useful help for further band assignment in vibrational spectra of these species.

4.2.1 The INS Spectra of NAM

Spectroscopy and diffraction experiments indicate the presence of pure HNO_3 , which is in accordance with the literature data. The reason for that is, on one hand, demixing according to the phase diagram, and on the other hand, the elevated vapour pressure of HNO_3 above the liquid. In general, molecular nitric acid tends to decompose into water and NO_2 , which has also been observed by spectroscopic means. The INS data exhibit a much higher quality and better spectral resolution than the literature data, Janik et al. (1968), and some new band positions of water torsions and oxonium hindered rotations have been observed. Further band assignment may be done in the future aided by theoretical models which can in turn be refined through the confirmation of calculated bands.

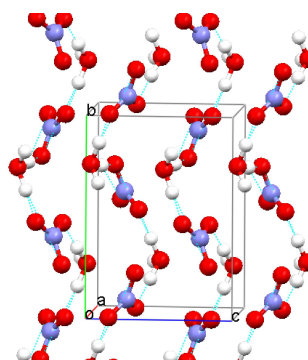


Figure 4.2: NAM structure generated from XRD-data.

4.2.2 The INS Spectra of NAT

The INS spectra of the NAT have been recorded for the first time here and they back up the State diagram of the nitric acid hydrates that was proposed by Tizek et al. (2004). The Figure 3.17 shows good and clearly distinguishable spectra. The spectrum has a good resolution especially in the low wavenumber region which is a characteristic of the TOSCA experiment through which the spectra were gained. Many bands can be distinguished which may serve further band assignment in the future. Once the bands are identified they can help in field measurement to guide the attention to such wavenumber regions which may enable the scientist to even distinguish between metastable phases by the use of spectroscopic methods. All these data may contribute to a better understanding of the building mechanisms of PSCs and also if man has an impact on this sensitive system.

4.2.3 Preparation Method

The preparation method explained in Section 2.2.2 was invented and used for the nitric acid samples here for the first time. Through its simple use and functionality this method may be a method of choice for the production of amorphous samples in the future. The problem of producing a sufficient amount of amorphous samples is often present in the research of metastable phases and also in many other fields of research where an initially amorphous sample is needed.

4.3 Outlook

Many processes involving ices in the atmosphere are still poorly understood. To make serious predictions of cloud behavior and properties this knowledge is essential. As long as this knowledge is not present it is hard to determine what impact mankind has on such sensitive systems. Some processes are understood, others can be observed but not explained, and most of the processes are probably still hidden from us.

Concerning the clouds, many inorganic compounds have been investigated in the past concerning their role in the cloud systems. The organic materials such as carboxylic acids and humic substances have not been in such a strong focus of research until recent years, even though they are ubiquitous in the atmosphere as well. At the moment many scientists direct their work to these organic compounds and their impact on ice nucleation.

The citric acid that was used in the investigations in this work was mainly used as a proxy for other carboxylic acids in the atmosphere. Citric acid itself has no strong relevance for cloud chemistry as it is just present to a minor extent. However, the amount of information that was already present on citric acid served well in order to become acquainted with the model system and the methods. Consequently, carboxylic acids which are present in relevant amounts in the atmosphere need to be investigated on their nucleation influences with similar, possibly refined methods. One of the next interesting substances would be oxalic acid, as it is sufficiently present in the atmosphere to have an impact on the cloud building mechanisms. Besides the carboxylic acids, the influence of many other organic compounds is still unknown. Such compounds as soluble humic substances and even solid biological material (e.g. pollen, bacteriae, funghi-spores,...) await further investigation in the future. Just recently Pratt et al. (2009) showed that 33% of the compounds found in cloud ice particles are of biologic origin. Even though this amount is large, only poor knowledge exists about these biological aerosol particles concerning their nucleation behaviour. Especially particles such as spores, pollen and bacteriae have very characteristic surfaces which serve their tasks in the lifecycle. As water is involved in most biological processes, it is an assumption that they also have a characteristic behaviour concerning water and perhaps also concerning ice.

Besides clouds, the understanding of water with its crystalline phases and its interac-

tion with other materials is a field of research that can be a source of understanding for a myriad of processes in the living as well as in the inanimate world. With the scientific methods available today it is possible to go much further into detail as was possible years ago. This opportunity should be used to reveal as much information as possible on one of the most important compounds for living beings.

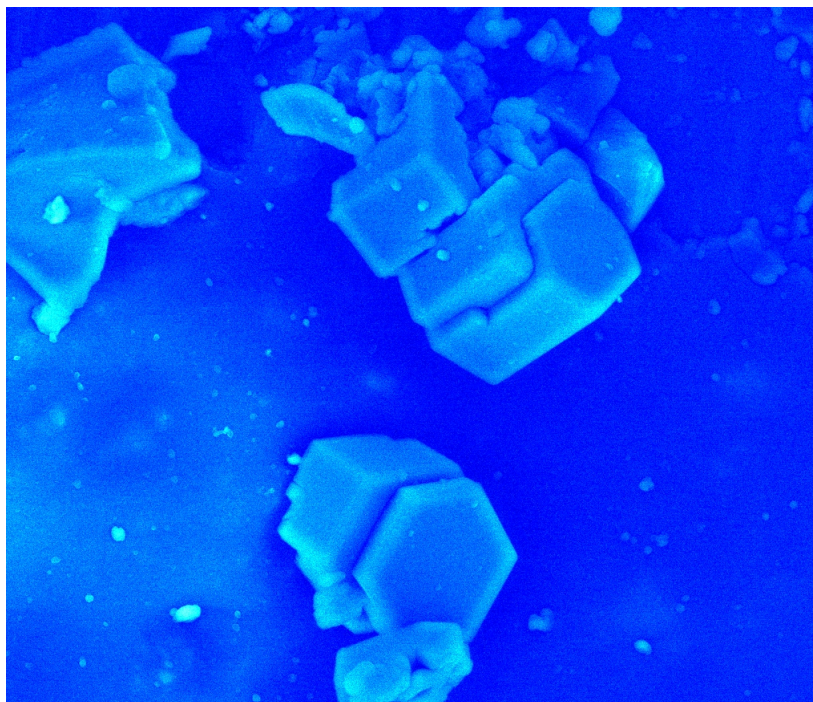


Figure 4.3: Falsecolor image of a beautiful hexagonal ice crystal observed with ESEM.

Bibliography

URL <http://www.britannica.com/EBchecked/topic/122305/cloud>.

URL <http://www.noaa.gov>.

- S. Arrhenius. On the Influence of Carbonic Acid in the Air upon the Temperature of the Ground. *Philosophical Magazine and Journal of Science*, 5, 41:237–276, 1896.
- A. Ashkin and J. M. Dziedzic. Optical Levitation of Liquid Drops by Radiation Pressure. *Science*, 187:1073–1075, 1975.
- M. B. Baker and T. Peter. Small-Scale Cloud Processes and Climate. *Nature*, 451: 299–300, 2008.
- N. Barton, B. Rowland, and J. P. Devlin. Infrared Spectra of Large Acid Hydrate Clusters: Formation Conditions of Submicron Particles of $\text{HNO}_3 \cdot 2\text{H}_2\text{O}$ and $\text{HNO}_3 \cdot 3\text{H}_2\text{O}$. *Journal of Physical Chemistry*, 97:5848–5851, 1993.
- B. S. Berland, D. R. Haynes, K. L. Foster, M. A. Tolbert, S. M. George, and O. B. Toon. Refractive Indices of Amorphous and Crystalline $\text{HNO}_3/\text{H}_2\text{O}$ Films Representative of Polar Stratospheric Clouds. *Journal of Physical Chemistry*, 98:4358–4364, 1994.
- D. E. Bethell and N. Sheppard. The Infrared Spectrum of the H_3O^+ Ion in Acid Hydrates. *Journal of Chemical Physics*, 21:1421, 1953.
- K. D. Beyer and A. R. Hansen. Phase Diagram of the Nitric Acid/Water System: Implications for Polar Stratospheric Clouds. *Journal of Physical Chemistry A*, 106: 10275–10284, 2002.
- C. Budke and T. Koop. Ice Recrystallization Inhibition and Molecular Recognition of Ice Faces by Poly(vinyl alcohol). *ChemPhysChem*, 7:2601–2606, 2006.
- P. J. Crutzen and F. Arnold. Nitric Acid Cloud Formation in the Cold Antarctic Stratosphere: A Major Cause for the Springtime "Ozone Hole". *Nature*, 324:651–655, 1986.

- R. G. Delaplane, I. Taesler, and I. Olovsson. Hydrogen Bond Studies.XCIII. Oxonium Ion in Nitric Acid Monohydrate. *Acta Crystallographica B*, B31:1486–1489, 1975.
- T. Dienes, O. Hollricher, and J. Toporski. *Confocal Raman Microscopy*. Springer Series in Optical Sciences. Springer, 2011.
- R. Escribano, M. Couceiro, P. C. Gómez, E. Carrasco, M. A. Moreno, and V. J. Herrero. The Nitric Acid Hydrates: Ab Initio Molecular Study, and RAIR Spectra of the Solids. *Journal of Physical Chemistry A*, 107:651–661, 2003.
- R. M. Escribano, D. Fernández-Torre, V. J. Herreiro, B. Martín-Llorente, B. Maté, I. K. Ortega, and H. Grothe. The Low Frequency Raman and IR spectra of Nitric Acid Hydrates. *Vibrational Spectroscopy*, 43:6, 2006.
- D. Fernández, V. Botella, V. J. Herrero, and R. Escribano. A Theoretical Study of the Structure and Spectra of Nitric Acid Hydrates Crystals. *Journal of Physical Chemistry B*, 107:10608–10614, 2003.
- D. Fernández-Torre and R. Escribano. First-Principles Infrared Spectrum of Nitric Acid and Nitric Acid Monohydrate Crystals. *Journal of Chemical Physics A*, 108: 10535–10541, 2004.
- D. Fernández-Torre, R. Escribano, V. J. Herrero, B. Maté, M. A. Moreno, and L. K. Ortega. Theoretical Calculations of Refractive Indices and Optical Effects in Spectra of Nitric Acid and Nitric Acid Monohydrate. *Journal of Physical Chemistry B*, 109: 18010–18017, 2005.
- J. B. J. Fourier. Remarques générales sur les Températures du Globe terrestre et des espaces planétaire. *Annales de Chimie et de Physique*, 27:136–167, 1824.
- H. Grothe, C. E. Lund Myhre, and C. J. Nielsen. Low-Frequency Raman Spectra of Nitric Acid Hydrates. *Journal of Physical Chemistry A*, 110:171–176, 2006a.
- H. Grothe, H. Tizek, D. Waller, and D. J. Stokes. The Crystallization Kinetics and Morphology of Nitric Acid Trihydrate. *PCCP*, 8:2232–2239, 2006b.
- T. Huthwelker, M. Ammann, and T. Peter. The Uptake of Acidic Gases on Ice. *Chemical Reviews*, 106;4:1375–1444, 2006.
- IPCC. *Climate Change 2007: The Physical Science Basis. Contribution of Working Group I to the Fourth Assessment Report of the Intergovernmental Panel on Climate Change*. Cambridge University Press, 2007.
- A. Janik, A. Bajorek, J. M. Janik, I. Natkaniec, K. Parlinski, and M. Sudnik-Hryniewicz. Neutron Inelastic Scattering Data for Crystalline $\text{H}_3\text{O}\cdot\text{NO}_3$, CH_3I , and CH_2I_2 and their Comparison with Infrared and Raman Spectroscopy. *Acta Physica Polonica*, 33:13, 1968.

- R. Jenkins and R. L. Snyder. *Introduction to X-ray powder Diffractometry*. Wiley-VCH, 1996.
- B. G. Koehler. Desorption Kinetics of Model Polar Stratospheric Cloud Films Measured Using Fourier Transform Infrared Spectroscopy and Temperature-Programmed Desorption. *International Journal of Chemical Kinetics*, 33(5):295–309, 2001.
- T. Koop, B. Luo, A. Tsias, and T. Peter. Water Activity as the Determinant for Homogeneous Ice Nucleation in Aqueous Solutions. *Nature*, 406:611–614, 2000.
- B. Kärcher and T. Koop. The Role of Organic Aerosols in Homogeneous Ice Formation. *Atmospheric Chemistry and Physics*, 5:703–714, 2005.
- N. Lebrun, F. Mahe, J. Lamiot, M. Foulon, J. C. Petit, and D. Prevost. Kinetic Behaviour Investigations and Crystal Structure of Nitric Acid Dihydrate. *Acta Crystallographica Section B*, B57:27–35, 2000.
- E. G. Lierke. Akustische Positionierung - Ein umfassender berblick über Grundlagen und Anwendungen. *Acoustica*, 82:220–237, 1996.
- M. P. McCormick, H. M. Steele, P. Hamill, W. P. Chu, and T. J. Swissler. Polar Stratospheric Cloud Sightings by SAM II. *Journal of the Atmospheric Sciences*, 39:1387–1397, 1982.
- A. M. Middlebrook, B. S. Berland, S. M. George, , M. A. Tolbert, and O. B. Toon. Real Refractive Indices of Infrared-Characterized Nitric-Acid/Ice Films: Implications for Optical Measurements of Polar Stratospheric Clouds. *Journal of Geophysical Research*, 99:12, 1994.
- O. Mishima. The Glass-to-Liquid Transition of the Emulsified High-Density Amorphous Ice Made by Pressure-Induced Amorphization. *Journal of Chemical Physics*, 121, 7:3161–3163, 2004.
- O. Mishima and H. E. Stanley. The Relationship Between Liquid, Supercooled and Glassy Water. *Nature*, 396:329–335, 1998.
- P. C. H. Mitchell, S. F. Parker, A. J. Ramirez-Cuesta, and J. Tomkinson. *Vibrational Spectroscopy with Neutrons*. World Scientific Publishing Co. Pte. Ltd., 2005.
- B. J. Murray. Inhibition of Ice Crystallisation in Highly Viscous Aqueous Organic Acid Droplets. *Atmospheric Chemistry and Physics*, 8:5423–5433, 2008a.
- B. J. Murray. Enhanced Formation of Cubic Ice in Aqueous Organic Acid Droplets. *Environmental Research Letters*, 3:1–7, 2008b.

- B. J. Murray, D. A. Knopf, and A. K. Bertram. The Formation of Cubic Ice under Conditions Relevant to Earth's Atmosphere. *Nature*, 434:202–205, 2005.
- W. Paul and M. Raether. Das Elektrische Massenfilter. *Zeitschrift für Physik*, 140: 262–273, 1955.
- S. Peil, S. Seisel, and O. Schrems. FTIR-Spectroscopic Studies of Polar Stratospheric Cloud Model Surfaces: Characterization of Nitric Acid Hydrates and Heterogeneous Reactions Involving N_2O_5 and HBr . *Journal of Molecular Structure*, 348:449–452, 1995.
- T. Peter, C. Marcolli, P. Spichtinger, T. Corti, M. B. Baker, and T. Koop. When Dry Air Is Too Humid. *Science*, 314:1399–1402, 2006.
- R. D. Poshusta and D. C. Tseng. Periodic Hartree-Fock Study of Nitric Acid Monohydrate Crystal: Bulk and Clean Surface. *Journal of Physical Chemistry*, 97:7295–7303, 1993.
- K. A. Pratt, P. J. DeMott, F. J. R., Z. Wang, D. L. Westphal, A. J. Heymsfield, C. H. Twohy, A. J. Prenni, and K. A. Prather. In Situ Detection of Biological Particles in Cloud Ice-Crystals. *Nature Geoscience*, 2:398–401, 2009.
- H. Reinhardt, M. Fida, and R. Zellner. DRIFTS- Studies of the Interactions of HNO_3 with Ice and HCl (HNO_3)- hydrate surfaces at temperatures around 165 K. *Journal of Molecular Structure*, 661-662:11, 2003.
- G. Ritzhaupt and P. J. Devlin. Infrared Spectra of Nitric and Hydrochloric Acid Hydrate Thin Films. *Journal of Physical Chemistry*, 95:90–95, 1991.
- M. Sato, O. Setokuchi, K. M. T. Yamada, and T. Ibusuki. Experimental Simulation of Infrared Spectra of PSCs: Films of Nitric Acid/Water-Ice Mixture at Low Temperatures Observed by Grazing-Angle Reflection Spectroscopy. *Vibrational Spectroscopy*, 31:167–172, 2003.
- R. Savoie and P. A. Giguere. Infrared Study of the Crystalline Monohydrates of Nitric, Perchloric, and Sulfuric Acids. *Journal of Chemical Physics*, 41:2698–2705, 1964.
- J. H. Seinfeld and S. N. Pandis. *Atmospheric Chemistry and Physics: From Air Pollution to Climate Change*. John Wiley and Sons, 1998.
- D. Skoog, F. Holler, and T. Nieman. *Principles of Instrumental Analysis*. Brooks/Cole Publishing Co., 2006.
- R. H. Smith, M.-T. Leu, and L. F. Keyser. Infrared Spectra of Solid Films Formed from Vapors Containing Water and Nitric Acid. *Journal of Physical Chemistry*, 95:5924–5930, 1991.

- J. L. Stanford and J. S. Davis. A Century of Stratospheric Cloud Reports: 1870-1972. *Bulletin American Meteorological Society*, 55:213–219, 1974.
- H. E. Stanley, S. V. Buldyrev, M. Canpolat, S. Havlin, O. Mishima, M. R. Sadr-Lahijany, A. Scala, and F. W. Starr. The Puzzle of Liquid Water: A Very Complex Fluid. *Physica D*, 133:453–462, 1999.
- H. E. Stanley, S. V. Buldyrev, M. Canpolat, O. Mishima, M. R. Sadr-Lahijany, A. Scala, and F. W. Starr. The Puzzling Behaviour of Water at Very Low Temperature. *PCCP*, 2:1551–1558, 2000a.
- H. E. Stanley, S. V. Buldyrev, O. Mishima, M. R. Sadr-Lahijany, A. Scala, and F. W. Starr. Unsolved Mysteries of Water in its Liquid and Glassy Phases. *Journal of Physics; Condensed Matter*, 12:A403–A412, 2000b.
- D. J. Stokes, B. L. Thiel, and A. M. Donald. Direct Observation of Water-Oil Emulsion Systems in the Liquid State by Environmental Scanning Electron Microscopy. *Langmuir*, 14:4402–4408, 1998.
- Y. Suzuki and O. Mishima. Raman Study of the Annealing Effect of Low-Density Glassy Water. *Journal of the Physical Society of Japan*, 72, (12):3128–3131, 2003.
- Y. Suzuki, Y. Takasaki, Y. Tominaga, and O. Mishima. Low-Frequency Raman Spectra of Amorphous Ices. *Chemical Physics Letters*, 319:81–84, 2000.
- H. Tizek, E. Knözinger, and H. Grothe. X-ray Diffraction Studies on Nitric Acid Dihydrate. *PCCP*, 4:5128–5134, 2002.
- H. Tizek, E. Knözinger, and H. Grothe. Formation and Phase Distribution of Nitric Acid Hydrates in the Mole Fraction Range $\text{HNO}_3 \leq 25\%$: A combined XRD and IR study. *PCCP*, 6:972–979, 2004.
- O. B. Toon, P. Hamill, R. P. Turco, and J. Pinto. Condensation of HNO_3 and HCl in the Winter Stratospheres. *Geophysical Research Letters*, 13(12):1284–1287, 1986.
- T. L. Tso and M. T. Leu. Quantitative Analysis of the Infrared Absorptivities of Nitric Acid Ices Aerosol Existing in Polar Stratospheric Clouds. *Analytical Sciences*, 12: 615–622, 1996.
- G. Tóth. Quantum Chemical Study of the Different Forms of Nitric Acid Monohydrate. *Journal of Physical Chemistry A*, 101:8871–8876, 1997.
- M. Walker, C. A. Morrison, and D. R. Allan. Nitric Acid Monohydrates at High Pressure: An Experimental and Computational Study. *Physical Review B*, 72: 224106(1–9), 2005.

- D. Waller. *Environmental Scanning Electron Microscopy of Freezing Aqueous Solutions*. PhD thesis, School of Physics, Cavendish Laboratory, Cambridge, 2007.
- D. Waller, D. J. Stokes, and A. M. Donald. Improvements to a Cryosystem to Observe Ice Nucleating in a Variable Pressure Scanning Electron Microscope. *Review of Scientific Instruments*, 79:103709(1–7), 2008.
- P. J. Wooldridge, R. Zhang, and M. J. Molina. Phase equilibria of H_2SO_4 , HNO_3 , and HCL hydrates and the Composition of Polar Stratospheric Clouds. *Journal of Geophysical Research*, 100:8, 1995.
- H. Yang and B. J. Finlayson-Pitts. Infrared Spectroscopic Studies of Binary Solutions of Nitric Acid and Water and Ternary Solutions of Nitric Acid, Sulfuric Acid, and Water at Room Temperature: Evidence for Molecular Nitric Acid at the Surface. *Journal of Physical Chemistry A*, 105:1890–1896, 2001.
- B. Zobrist, C. Marcolli, T. Koop, B. P. Luo, D. M. Murphy, U. Lohmann, A. A. Zardini, U. K. Krieger, T. Corti, D. J. Cziczo, S. Fueglistaler, P. K. Hudson, D. S. Thomson, and T. Peter. Oxalic Acid as a Heterogeneous Ice Nucleus in the Upper Troposphere and its Indirect Aerosol Effect. *Atmospheric Chemistry and Physics*, 6:3115–3129, 2006.
- B. Zobrist, C. Marcolli, D. A. Pedernera, and T. Koop. Do Atmospheric Aerosols form Glasses? *Atmospheric Chemistry and Physics*, 8:5221–5244, 2008.